

**PHYSICAL AND MECHANICAL PROPERTIES OF PALM
KERNEL ACTIVATED CARBON AFTER IMMERSE IN
DIFFERENT TYPES OF VEGETABLES OIL**



UNIVERSITI TEKNIKAL MALAYSIA MELAKA

**PHYSICAL AND MECHANICAL PROPERTIES OF PALM KERNEL
ACTIVATED CARBON AFTER IMMERSE IN DIFFERENT TYPE OF
VEGETABLES OIL**

AFIQ TAQUIDDIN BIN KAMARUSZAMAN



UNIVERSITI TEKNIKAL MALAYSIA MELAKA

2022

DECLARATION

I declared that this project entitled “Physical and mechanical properties of palm kernel activated carbon (PKAC) after immerse in different type of vegetables oil.” is the result of my own work except as cited in the references.



APPROVAL

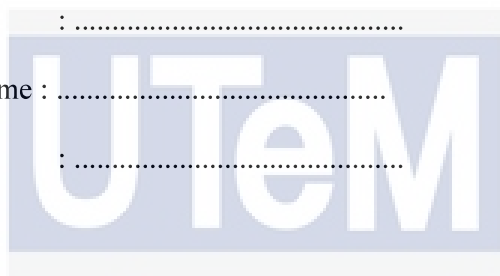
I hereby declare that I have read this project report and in my opinion this report is sufficient in terms of scope and quality for the award of the degree of Bachelor Mechanical Engineering



Signature :

Supervisor's Name :

Date :



اونيورسيتي تیکنیکل ملیسیا ملاک

UNIVERSITI TEKNIKAL MALAYSIA MELAKA

DEDICATION

To my beloved mother and father



ABSTRACT

Palm kernel activated carbon (PKAC) found that become one of the potential self-lubricant materials. Agricultural wastes would be preferred for use in activated carbon industries since they are both cost effective and environmentally favourable. In Malaysia, huge amount of palm kernel is producing as agricultural wastes. low friction coefficient, palm kernel activated carbon reinforced polymeric composite can replace existing high-cost industrial self-lubricated materials. In this project the effect of immersing in different type of vegetables oil on physical and mechanical properties of palm kernel activated carbon reinforced with polymeric composites was investigated. The composition of 60%, 65% and 70% of the weight activated carbon was reinforced with the polymer resin and compacted into a die at 100°C with 1225kPa pressure for 10 minutes by using compaction technique. Three type shape prepared which is disc, pin and bone for conducting of tensile (ASTM D3039 / D3039M-17), compression (ASTM D 6641), hardness (ASTM D2240-15e1), surface roughness, density, porosity and water absorption (ASTM D570-98(2010) e1) tests. All the test conducted before and after immersing in three types of vegetables oil which is soybean, palm, and corn oil. The 60% sample had the most excellent properties in terms of hardness, surface roughness, tensile and compression. Immersing in different types of vegetables oil give slightly difference physical and mechanical properties of the composites compared to before immersed.

ABSTRAK

Karbon aktivasi isirong kelapa sawit didapati menjadi salah satu bahan yang berpotensi sebagai pelincir sendiri. Kegunaan bahan buangan hasil dari pertanian memberi keuntungan dalam industri aktivasi karbon yang mana ia lebih ekonomi dan mesra alam. Di Malaysia, banyak isirong kelapa sawit yang terhasil sebagai bahan buangan pertanian. Disebabkan oleh pekali geseran rendah, karbon aktivasi isirong kelapa sawit diperkuatkan dengan komposit polimer boleh menggantikan bahan pelincir sendiri yang sedia ada dalam industri yang mempunyai kos yang lebih tinggi. Di dalam projek ini, kesan setelah direndam didalam beberapa jenis minyak sayur terhadap karbon aktivasi biji kelapa sawit yang diperkuatkan dengan polimer komposit telah dijalankan ujian terhadapnya. Beberapa komposisi PKAC seperti 60%, 65% dan 70% dari berat aktivasi karbon diperkuatkan dengan damar polimer dimampatkan didalam acuan dan dipanaskan pada 100 darjah Celsius serta 1225kPa tekanan selama 10 minit dengan menggunakan teknik pemadatan. Tiga jenis bentuk yang disediakan bagi mencapai objektif projek ini antaranya adalah cakera, pin dan tulang. Untuk menjalankan ujian tegangan (ASTM D3039 / D3039M-17), pemampatan (ASTM D 6641), kekerasan (ASTM D2240-15e1), kekasaran permukaan, ketumpatan, keliangan dan penyerapan air (ASTM D570-98(2010) e1). Kesemua ujian yang dijalankan semasa sebelum dan rendam didalam tiga jenis minyak sayur antaranya adalah kacang soya, kelapa sawit dan jagung. Komposisi 605 didapati sebagai yang terbaik dalam ujian kekerasan, kekasaran permukaan, ketegangan dan pemampatan. Merendam dalam beberapa jenis minyak sayur memberikan sedikit perubahan dalam ciri-ciri fizikal dan mekanikal komposit jika dibandingkan dengan sebelum direndam didalam minyak sayur.

ACKNOWLEDGEMENT

First and foremost, I would like to thank God to whom all praise is due. without His permission, nothing is possible. I would also like to express my sincere gratitude to my supervisor, Dr. Mohd Rody bin Mohammad Zin from the Faculty of Mechanical Engineering Universiti Teknikal Melaka (UTeM) for his dedication and great interest above all his overwhelming attitude towards the completion of this project report.

I owe a deep sense of thanks to the panels Dr. Wan Mohd Farid bin Wan Mohamad and Dr. Siti Hajar binti Sheikh Md. Fadzullah during the seminar session which they gave constructive comments toward my study and suggestion to improve my project.

Particularly, I would also like to express my gratitude to post graduate student Nur Aqila Syamimi binti Amir Hamzah, who have been helping and giving advice on my work. Not to forget, Mrs Hidayah, the technician from tribology lab which have given guidance during conducting the experiment. Thanks also to Faculty of Mechanical Engineering UTeM in funding me the cost for this project.

Special thanks to my parents, siblings, and friends for their moral support in completing this bachelor's programme.

TABLE OF CONTENTS

	PAGE
DECLARATION	
APPROVAL	
DEDICATION	
ABSTRACT	i
<i>ABSTRAK</i>	ii
ACKNOWLEDGEMENT	iii
TABLE OF CONTENT	iv
LIST OF TABLES	vi
LIST OF FIGURES	viii
LIST OF APPENDICES	xii
LIST OF ABBREVIATIONS	xiii
CHAPTER	
1. INTRODUCTION	1
1.0. Background of study	1
1.1. Problem Statement	3
1.2. Objective	4
1.3. Scope	4
1.4. General methodology	5
2. LITERATURE REVIEW	7
2.0. Introduction	7
2.1. Tribology study	7
2.1.1. Tribology in brake system.	15
2.2. Solid lubricant	16
2.2.1. Diamond like carbon	17
2.2.2. Graphite.	19
2.3. Palm Kernel Activated Carbon	20
2.3.1. Physical properties PKAC.	22

2.3.2.	Mechanical properties of PKAC	26
2.4.	Vegetables oils.	28
2.4.1.	Tribology and Applications of Vegetable Oils	31
3.	METHODOLOGY	33
3.0.	Introduction.	33
3.1.	Sample preparation.	34
3.2.	Physical properties test.	41
3.3.	Mechanical properties.	43
3.4.	Immersing in different type of vegetable oil.	44
4.	RESULTS AND DISCUSSION	46
4.0.	Introduction	46
4.1.	Hardness.	46
4.2.	Surface roughness.	49
4.3.	Density	52
4.4.	Water absorption.	55
4.5.	Porosity.	59
4.6.	Tensile test.	61
4.7.	Compression test.	65
5.	CONCLUSION AND RECOMMENDATION	70
	REFERENCES	71
	APPENDICES	79

LIST OF TABLES

TABLE	TITLE	PAGE
3-1	Amount of PKAC and Epoxy for disc shape sample.	39
3-2	Amount of PKAC and Epoxy for pin shape sample.	39
3-3	Amount of PKAC and Epoxy for bone shape sample.	40
4-1	Hardness for disc before immersion in different type of vegetables oil.	47
4-2	Hardness for disc after immersion in different type of vegetables oil.	48
4-3	Surface roughness for disc before immersion in different type of vegetables oil.	50
4-4	Surface roughness of disc after immersion in different type of vegetables oil.	51
4-5	Density of disc before immersion in different type of vegetables oil.	53
4-6	Density of disc after immersion in different type of vegetables oil.	54
4-7	Water absorption of disc before immersion in different type of vegetables oil.	56
4-8	Water absorption of Disc after immersion in different type of vegetables oil.	57
4-9	Porosity for disc sample.	59
4-10	Tensile strain.	61

4-11	Tensile stress.	62
4-12	Young modulus for tensile test.	63
4-13	Compressive strain.	66
4-14	Compressive stress.	67
4-15	Young modulus for compression test.	68



LIST OF FIGURES

FIGURE	TITLE	PAGE
1-1	Flow chart of project.	6
2-1	Abrasives wear mechanism. (Roger Lewis & Olofsson, 2009)	10
2-2	Wear rates of R8T wheel material versus slip (–) using a twin-disc rolling /sliding test. (R. Lewis & Dwyer-Joyce, 2004)	10
2-3	UIC60 900A rail steel wear map. (R. Lewis & Olofsson, 2004)	11
2-4	Form change of wheel and rail over a two-year period from the Stockholm test case. (Roger Lewis & Olofsson, 2009)	12
2-5	Creep curves generated by twin-disc testing. (Hardwick et al., 2014)	12
2-6	Ideal friction coefficients in the wheel–rail contact for heavy haul traffic. (Zhu, 2011)	13
2-7	Technical disc brake, principle and frictional force. (Ostermeyer & Müller, 2008)	15
2-8	Coefficient of friction of graphite (a) and graphene (b) in different atmospheres. (Berman et al., 2014)	20
2-9	Hardness of palm kernel activated carbon reinforced polymeric composite at room temperature and at 90°C. (Mohmad et al., 2018)	23
2-10	Density of palm kernel activated carbon reinforced polymeric	24

	composite at different compositions. (Mohmad et al., 2018)	
2-11	Porosity of palm kernel activated carbon reinforced polymeric composite at different compositions. (Mohmad et al., 2018)	25
2-12	Average elastic modulus of palm kernel activated carbon reinforced polymeric. (Mohmad et al., 2018)	27
2-13	Average ultimate tensile strength of palm kernel activated carbon reinforced polymeric. (Mohmad et al., 2018)	27
2-14	Schematic representation of a triglyceride molecule.	28
2-15	Schematic representation of a saturated fatty acid.	29
2-16	Schematic representation of (a) monounsaturated and (b) polyunsaturated fatty acids	29
2-17	Schematic representation of a hydroxy fatty acid.	30
2-18	Schematic representation of an Epoxy fatty acid.	31
2-19	Variation of coefficient of friction and wear rate for vegetable oils. (Reeves et al., 2012)	32
3-1	Flow Chart for Experiment.	33
3-2	Palm Kernel Activated Carbon (PKAC).	34
3-3	West System 105 Epoxy Resin.	34
3-4	West System 206 Slow Hardener.	35
3-5	Crusher machine.	35
3-6	Sieving machine.	36
3-7	250 μ m in size of PKAC.	37
3-8	Mould for disc shape.	37
3-9	Mould for bone shape.	37

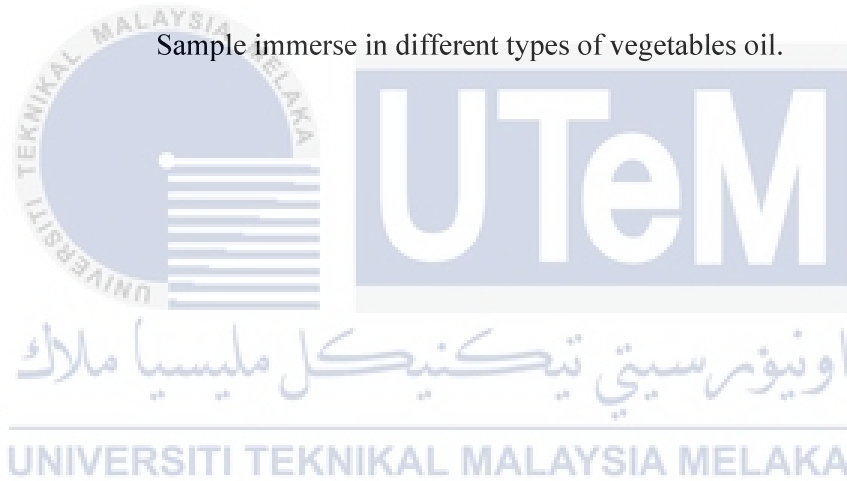
3-10	Mould for pin shape.	38
3-11	Hot press machine.	38
3-12	Weight scale.	41
3-13	Shore Hardness Durometer-D.	41
3-14	Surface roughness tester profilometer.	42
3-15	Electronic densitometer.	42
3-16	Instron universal testing machine.	43
3-17	Palm oil.	44
3-18	Corn oil.	44
3-19	Soya oil.	45
4-1	Hardness of disc before immersion in different type of vegetables oil.	47
4-2	Hardness of Disc after immersion in different type of vegetables oil.	48
4-3	Surface roughness of disc before immersion in different type of vegetables oil.	50
4-4	Surface roughness of disc after immersion in vegetables oil.	51
4-5	Density of disc before immersion in different type of vegetables oil.	53
4-6	Density of disc after immersion in different type of vegetables oil.	54
4-7	Water absorption of disc before immersion in different type of vegetables oil.	56
4-8	Water absorption of disc after immersion in different type of vegetables oil.	57
4-9	Porosity for disc sample.	60
4-10	Tensile strain.	62
4-11	Tensile stress.	63

4-12	Young Modulus for tensile test.	64
4-13	Strain for compression test.	66
4-14	Compression stress.	67
4-15	Young modulus for compression test.	68



LIST OF APPENDICES

APPENDIX	TITLE	PAGE
A1	Sample after tensile test.	80
A2	Sample after compression test.	81
A3	Sample immerse in different types of vegetables oil.	82



LIST OF ABBREVIATIONS

PKAC - Palm Kernel Activated Carbon

COF - Coefficient of Friction

DLC - Diamond Like Carbon

LCF - Low Coefficient Friction

ASTM - American Society for Testing and Material

HPF - High Positive Friction

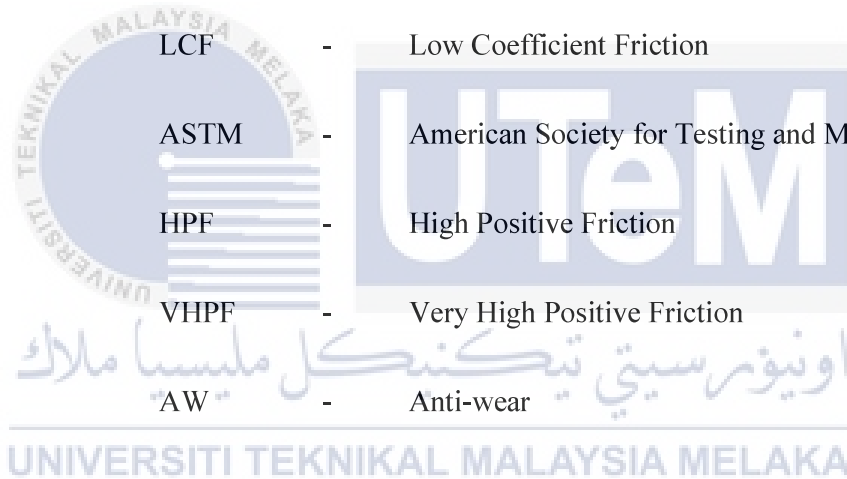
VHPF - Very High Positive Friction

AW - Anti-wear

EP - Extreme Pressure

LEO - Low Earth Orbit

3D - 3-Dimensional



CHAPTER 1

INTRODUCTION

1.0. Background of study.

Tribology is science of friction, wear, and lubrication. The word of tribology is derived from the Greek word *tribos* which means rubbing and friction. Tribological inventions are framed within time periods ranging from the prehistoric epoch (the stone age) to 3500 B.C., when one of the first examples of tribological applications was the generation of fire by friction between two pieces of wood. The tribology named officially arises from Jost Report. Tribology is the science and technology of interacting surfaces in relative motion and of the practices related thereto. (Jost, 1966), but tribological concepts, as for instance the way to reduce friction using rolling elements and lubricants, are much older than industry (Frêne et al., 1997; Dowson, 1998). Tribology is highly interdisciplinary involving many research fields as physics, mathematics, chemistry, materials science and engineering, and therefore connecting basic and applied sciences.

Friction is when two surfaces are making contact that produce energy, heat, and make the surface wear. The application of lubrication is to improve energy efficiency and mechanical reliability. Previous tribology research has yielded some promising wear-control methods, such as film coating, multi-phase alloying, and composite structuring, as well as lubrication. (Tahir et al., 2015). Solid lubrication, once considered an art form, has evolved into an important part of materials science and engineering. For a long time, companies have

used solid lubricating materials to achieve low friction and wear under a variety of conditions. Enhancing the tribology performance of solid lubricant materials will significantly reduce costs while also enhancing the efficiency of the machining method. (Shankar et al., 2017). Carbon has sparked the most interest among solid lubricants because of its unique properties. Carbon exists in a variety of ways, each with its own set of properties based on its particular structure (Lettington, 1998).

Palm kernel shells containing high carbon (50.01%) can be used as a precursor to produce activated carbon. (Mak et al., 2009). Physical or chemical activation carbon may be modified to produce activated carbon with high porosity and surface area. (Hadoun et al., 2013). Activated carbon is a carbonaceous substance that is mostly amorphous in nature but develops a high degree of porosity during the production and treatment process. Every activated carbon has a memory that is influenced by the source and the conditions of preparation. (Guzel F. and Uzum I, 2002) Almost any carbonaceous material can be used to make activated carbon. Agricultural wastes, on the other hand, are the most readily available and least expensive of all known raw materials. Since activated carbon is a cheap adsorbent, it is commonly used (Joshi et al., 2013). In this industrial revolution 4.0 era, environmental pollution became an issue with a great impact on social commitment in the last years, the need and demand for activated carbons is growing continuously. Because of its low friction coefficient, palm kernel activated carbon reinforced polymeric composite has the ability to replace existing high-cost industrial self-lubricated materials. At various temperatures and loads, palm kernel activated carbon reinforced polymeric composite has good tribological properties with high friction resistance and low wear rate. (Mat Tahir et al., 2016).

1.1. Problem statement.

The projecting edge or rim on the circumference of a steel wheel that is designed to hold the wheel on a rail is referred to as a flange. When transporting loads between fixed locations on a regular basis, rail transportation with flanged wheels is ideal. Loads may be made up of individuals, raw materials, or finished goods. Metal tracks provide low-friction movement, high-loading capability, and long-term durability. They are often self-contained and do not need the assistance of a driver. The wheels on a car or a shopping cart require a different level of precision and design than flanged wheel rail installations. To provide traction on flat surfaces, rubber or plastic tyres are made from softer materials. Metal wheels used on tracks, on the other hand, depend on precise geometry and engineering to stay on track.

Since the forces produced by contact between wheel and rail are dependent on the friction (or creep force) characteristics, friction conditions between wheel and rail play an important role in car dynamic action. For climbing a slope or braking near a station, for example, a high coefficient of friction (COF) is necessary. High COF, on the other hand, is not desirable for a car passing through a tight curve because it causes lateral force squeak noises and rail corrugation. (Tomeoka et al., 2002)

Friction control between wheel and rail has been used for many years, with sand being used to help a locomotive climb mountain, grease lubricant being used in tight curves to avoid corrugation or wheel-flange wear, and so on. However, even when using these techniques, COF may be set to a high or low level in a step-like manner. Too low or too high a COF causes wheel or rail problems, such as braking skids, station overruns, wheel/rail wear, and corrugation. (Tomeoka et al., 2002)

The heat generated in the contact zone between a wheel and a rail, as well as the increased temperature of the working surfaces, causes changes in the structure and mechanical properties of working bodies. It causes contact surface wear, which contributes to wheel flange and rail premature failure. (Descartes et al., 2011). The aim of lubricating the contact between the active rail gauge corner and the wheel flange is to minimise wheel and rail deterioration and thus wear. It must also ensure protection by reducing friction in curves to prevent wheel lift and, as a result, derailment. (Descartes et al., 2011) . One of the ways to reduce wear processes of surfaces in the flange contact is the application of lubrication devices for working surfaces. (Spiryagin et al., 2010)

1.2. Objective.

The objective of this study is:

- To study physical and mechanical properties of Palm Kernel Activated Carbon (PKAC) before and after immersion in different type of vegetable oil.
- To study the application of PKAC as solid lubricant for wheel flange railways.

1.3. Scope.

The study covers the physical and mechanical properties of palm kernel activated carbon (PKAC) before and after immersing in different types of vegetables oil. Hardness, surface roughness, density, weight, porosity, tensile and compression test were conducted in order to observe the effect of vegetables oil to PKAC. Making comparison of their properties between both before and after immersion in vegetables oil.

1.4. General Methodology

a. Literature review.

Collect information from previous studies journal, article, book and any related reference about the project.

b. Sample preparation.

Disc, pin and bone shape with composition of 70%, 65% and 60% of palm kernel activated carbon (PKAC) mixed with epoxy and hardener going through moulding process by using compacting technique using hot press machine with 100°C of temperature with pressure of 120kPa.

c. Experiment.

The experiment will focus on physical and mechanical properties test such as hardness, surface roughness, density, water absorption and porosity for disc shape sample, tensile for bone shape and compression for pin shape sample. The experiment conduct before and after immersing in different type of vegetables oil, which is palm, soybean, and corn oil. The duration of immersion is 24 hours.

d. Thesis writing.

A complete thesis will be written including all the data and results from the experiment. The general methodology of this study is simplified in the flow chart as shown in figure 1.1.

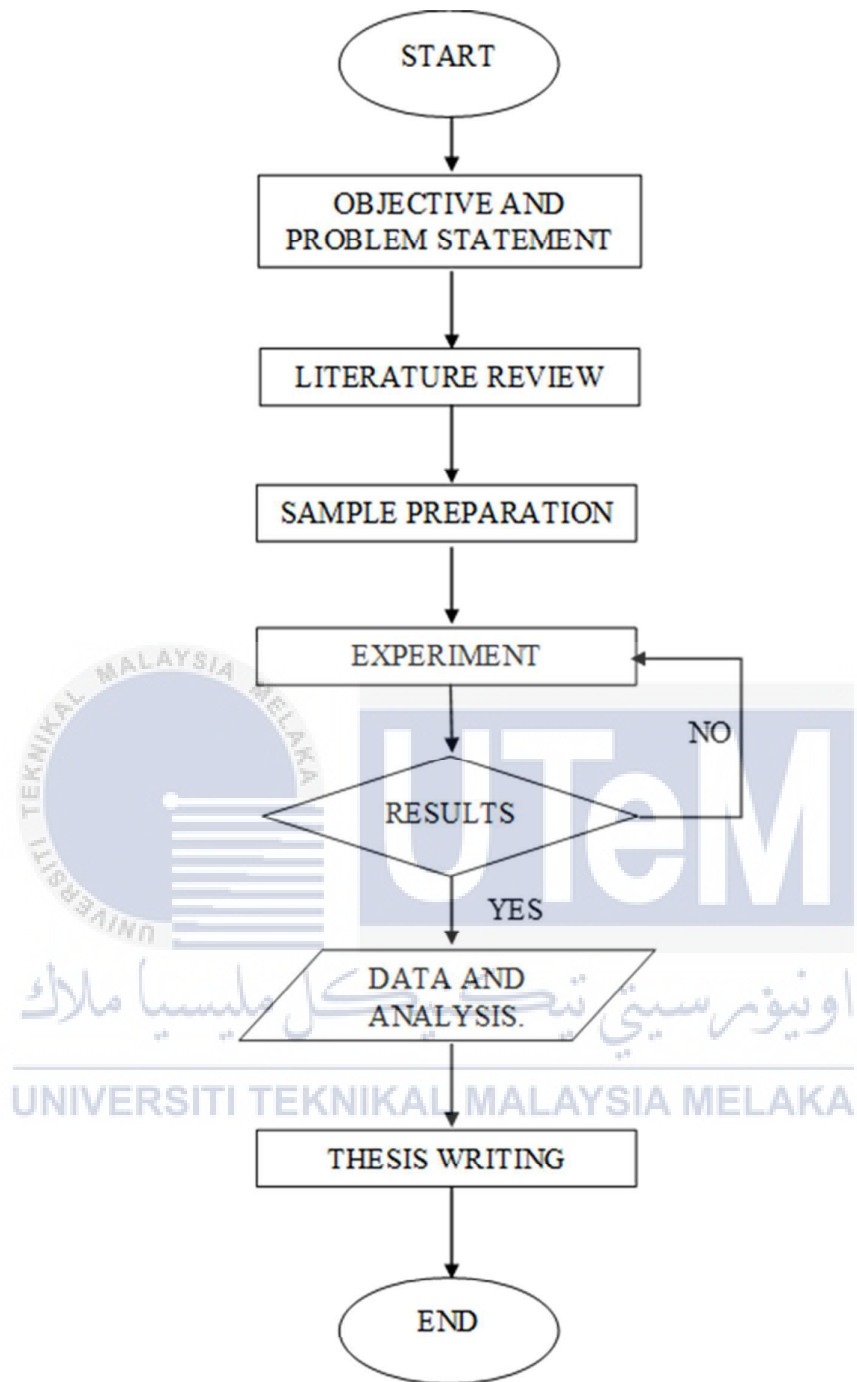


Figure 1-1: Flow chart of project.

CHAPTER 2

LITERATURE REVIEW

2.0. Introduction.

This chapter reviews previous research and study obtained from various source such as journals, articles, books, and web sites to find information related to this study. The purpose of this chapter is to create a guideline from previous study to complete this final year project. The information collected based on the objectives of this study. For instance, the information about tribological studies, solid lubricant, and PKAC are acquired to achieve the objectives.

This chapter is organized as follows. Section 2.2 describes on tribological studies. Section 2.3 about solid lubricant while section 2.4 explaining wheel flange lubricant. Section 2.5 continues with Palm Kernel Activated Carbon (PKAC).

2.1. Tribology study.

Tribology means the control and management of friction and wear, wherever it occurs. H.P. Jost, chairman of a group of British lubrication engineers, coined the term in 1966 to characterise the scientific and technical disciplines concerned with the study of friction, wear, and lubrication phenomena. However, the word tribology was unfamiliar to many people even to some in science and engineering since the 1990s (Blau PJ, 2009). Since

the time of Aristotle (384–322 BC), the topic of friction and wear has piqued the interest of renowned scientists. Only until the enormous breakthroughs that followed the industrial revolution in the early 18th century did we get a true grasp of wear and friction processes. Tribology has a strong link to long-term sustainability. By producing environmentally friendly lubricants, it can increasingly contribute to energy savings, pollution reduction, and reduced friction and wear losses. (Tzanakis et al., 2012). Investigations in numerous nations have quantified and enunciated the benefits of tribology, particularly sustainable tribology, the most renowned of which is the Chinese report (Jost HP, 2010). The enormous potential for economic and environmental advantages around the world demonstrates the relevance of tribology in lowering global carbon emissions. In the realm of tribology and surface engineering, certain advanced approaches are now being employed to decrease friction and wear to the bare minimum. (Najar, 2017).

2.1.1. Tribology in wheel flange.

In the service process of wheel and rail interaction, it is commonly accepted that railway wheels and rails experience surface damage such as wear and rolling contact fatigue. The purpose of lubricating the contact between the active rail gauge corner and the wheel flange is to reduce wheel and rail degradation and therefore wear. It must also assure safety by minimising friction in curves in order to prevent wheel raising and, as a result, derailment. Although rail and wheel lubrication and material improvements have significantly reduced the wear rate of both elements, wear may still be a significant issue, particularly in high freight railroads, sharp curves, and in the event of lubrication failure. The cost of rail maintenance is largely accounted for by the wear of the wheel flange and rail gauge corner. (Jin et al., 2011)

The heat generated in the contact zone between a wheel and a rail, as well as the increased temperature of the working surfaces, causes changes in the structure and mechanical properties of working bodies. It causes contact surface wear, which contributes to wheel flange and rail early failure. (Spiryagin et al., 2010). The loss or displacement of material from a contacting surface is known as wear. Debris can be a kind of material loss. Material displacement can occur as a result of adhesion or local plastic deformation of material from one surface to another. There are a variety of wear mechanisms that can occur between contacting bodies, each of which results in a variable rate of wear. Mild wear and severe wear are the most basic classifications for the many types of wear that result in varied wear rates. Mild wear leaves a smooth surface, which is typically smoother than the original. Severe wear, on the other hand, results in a rough surface that is often harsher than the original. (Ulf Olofsson et al., 2013)

Abrasive wear caused by hard particles between the contacting surfaces can also cause significant wear and reduce the life of the contacting bodies (Nilsson et al., 2006). Abrasive wear is damage to a component surface caused by the motion of either harder asperities relative to that surface (two-body abrasive wear) or hard particles trapped between the surfaces (three-body abrasive wear) (Figure 2-1). Such particles could have been injected between the two softer surfaces as a contaminant from the outside world, or they may have grown in situ by oxidation or another chemical or mechanical process.

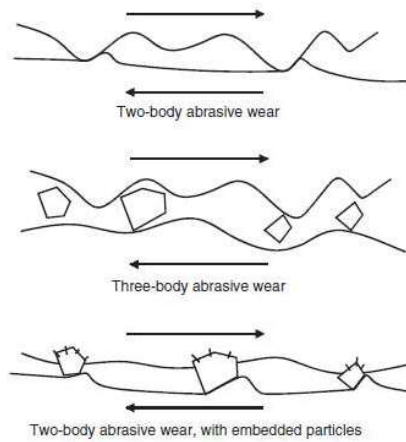


Figure 2-1: Abrasives wear mechanism. (Roger Lewis & Olofsson, 2009)

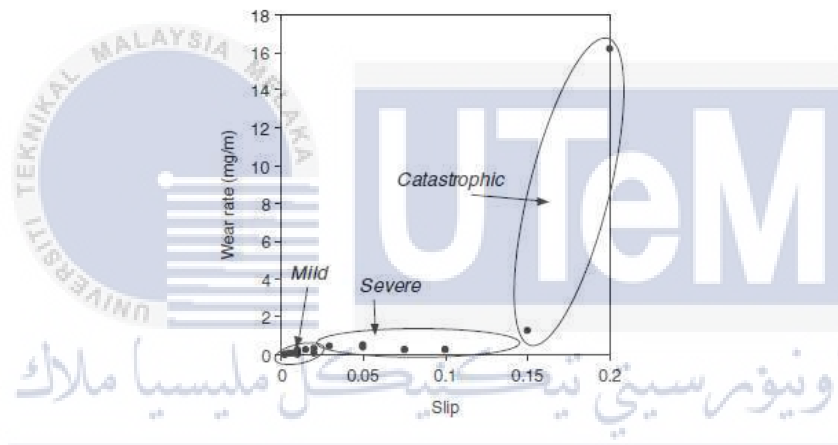


Figure 2-2: Wear rates of R8T wheel material versus slip (-) using a twin-disc rolling/sliding test. (R. Lewis & Dwyer-Joyce, 2004)

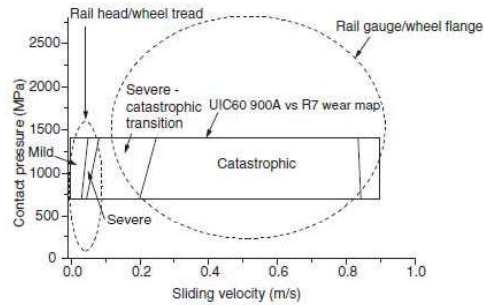


Figure 2-3: UIC60 900A rail steel wear map. (R. Lewis & Olofsson, 2004)

As illustrated in Figure 2-2 for R8T wheel material, the three wear regimes indicated above were observed during rolling/sliding laboratory experiments on wheel and rail materials. A map, such as the one shown in Figure 2-3, is a suitable way to represent wear data. A wheel–rail interaction is depicted on the map below. (R. Lewis & Olofsson, 2004). Using R7 wheel material and UIC 60 900A rail material, wear data was compiled using a combination of twin-disc and pin-on-disc testing methods. The map was placed on top of some expected wheel–rail contact circumstances. The wheel tread/railhead contact, as can be observed, is in the mild to severe wear range, while the wheel flange/rail gauge corner contact is in the severe to catastrophic. This corresponds to what has been observed in the field. In the contacting zone of a wheel–rail contact, both rolling and sliding occur. On the track side of the railhead, there can be a significant sliding component, especially in curves (gauge corner). Wear develops in the contact as a result of this sliding in the weakly lubricated condition that is typical of wheel–rail contact, as seen in Figure 2-4. In the case of sliding wear, an increase in the severity of loading (normal load, sliding velocity, or bulk temperature) leads to an abrupt shift in the wear rate at some point (volume loss per sliding distance). (Ulf Olofsson et al., 2013)



Figure 2-4: Form change of wheel and rail over a two-year period from the Stockholm test case. (Roger Lewis & Olofsson, 2009)

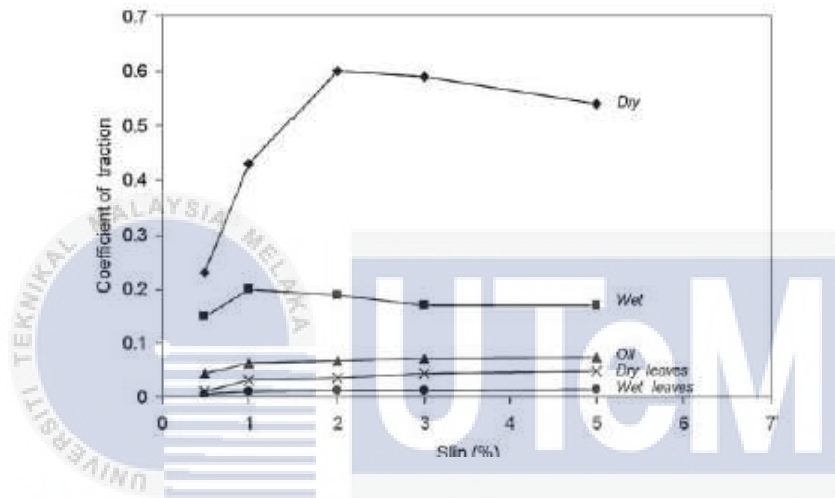


Figure 2-5: Creep curves generated by twin-disc testing. (Hardwick et al., 2014)

Controlling longitudinal creep or altering the friction level between the wheel and the rail can help improve wheel–rail adhesion. The link between the adhesion coefficient and creep is depicted in Figure 2-5 by the creep curve. Controlling the creep can help achieve a desired adhesion coefficient, depending on the demand. If the contact is polluted and a high level of adhesion is required, the creep should be carefully managed to achieve the highest adhesion coefficient, which is the saturation point in Figure 2-5. This is normally accomplished in the car using a slide control approach. (Andersson E, Berg M). The friction coefficient, on the other hand, is a critical element in determining the amount of available adhesion. Because of the high sliding speeds and heat generated at the interface, if the

friction coefficient is too low, the wheel will tend to slip under acceleration or lock under braking, causing damage to both the wheel and the rail. Excessive wear can also be caused by excessive friction. To keep the friction coefficient between the wheel and the rail at an acceptable level, friction management can be used. Figure 2-6 depicts the optimal friction coefficient for heavy load transportation. In order to obtain a target friction coefficient, FMs are applied to the wheel–rail interface. According to (Kalousek and Magel, 1997) they are divided into three categories:

- low coefficient friction modifier (LCF)/lubricant in the wheel flange/rail gauge contact.
- high positive friction modifier (HPF) in the wheel tread/railhead contact.
- very high positive friction modifier (VHPF) for locomotives.

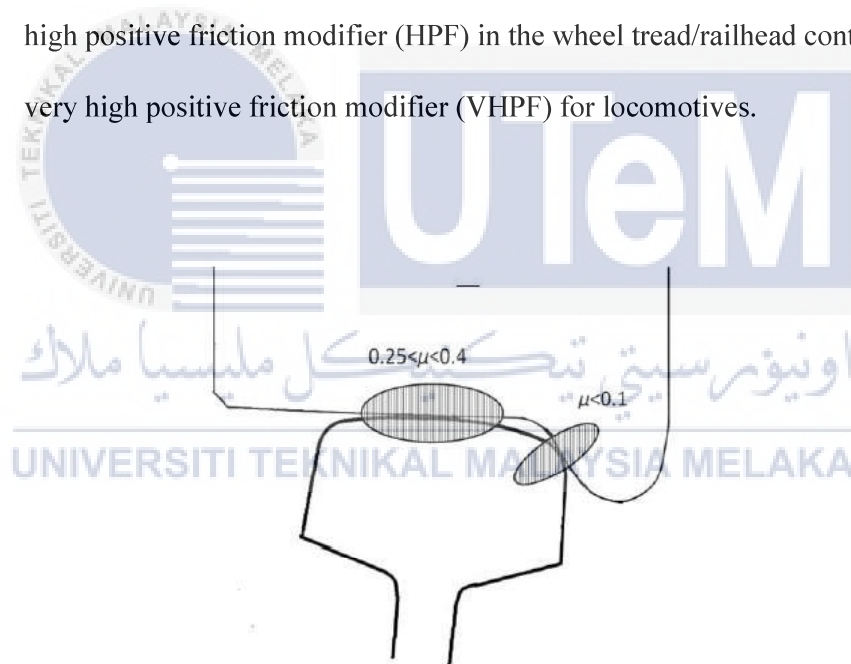


Figure 2-6: Ideal friction coefficients in the wheel–rail contact for heavy haul traffic. (Zhu, 2011)

Solids, oils, and greases can all be used to make LCF. When the train enters a curve and the wheel–rail contact switches from the railhead/wheel tread to the rail gauge/wheel flange, these lubricants are frequently applied to the hi-rail. Because the contact conditions between the wheel flange and the rail gauge are so harsh, LCF reduces the friction coefficient, minimising wear and noise. However, because friction levels in this location must be kept relatively high, it is critical that these LCFs do not migrate onto the railhead. Solid LCFs have an advantage here because a solid coating forms on the wheel flange and rail gauge. The advantages of rail lubricants in terms of lowering the friction coefficient are described in this article (U. Olofsson & Telliskivi, 2003) from field measurements and (Sundh & Olofsson, 2008) from laboratory tests.



2.1.1. Tribology in brake system.

Every day, nearly a million brake systems are made around the world. Calipers, discs, pads, and a variety of other devices fall under this category. As a result, their development is of great economic importance, particularly in terms of cost and durability. In the 1980s, many countries banned the use of asbestos fibres in brake pad compositions, ushering in a new era for the development of automotive brake pad materials. Asbestos fibre has a great resistance to mechanical, thermal, and chemical stresses, and as a result of these properties, it was a common component in brake pads. It was phased out for health reasons, and other substances had to take its place. The main requirements for brake pads are maximum coefficient of friction, a stable coefficient of friction (no immoderate fading; no variations under constant conditions), a minimum wear rate for the pad and disc, a minimum of aggressive wheel dust, stability against noise generation and other vibrations (squealing and judder) and low costs.

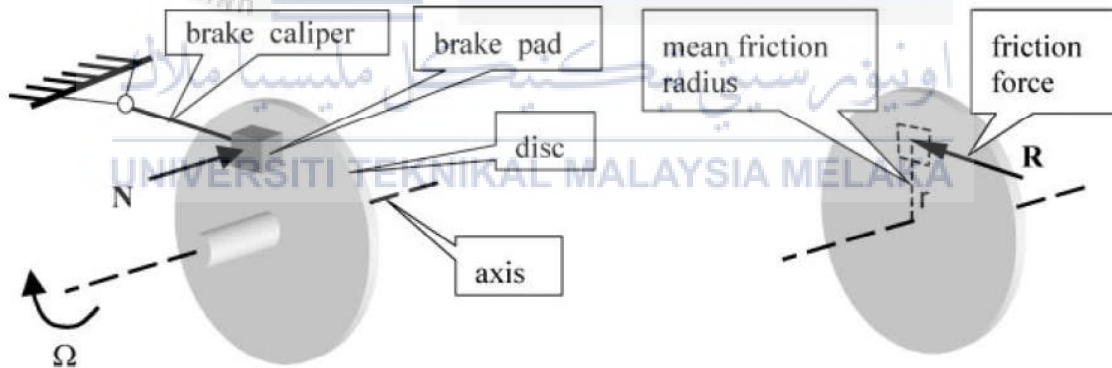


Figure 2-7: Technical disc brake, principle and frictional force. (Ostermeyer & Müller, 2008)

The general operation of a technological disc brake is depicted schematically in Figure 2-7. To apply the greatest feasible braking torque to an axis (rotational frequency V),

brake pads are pressed against a disc (connected to the axis) with the normal force N . The friction force R between the pad and the disc creates a brake torque $M=Rr$ (where r is the mean friction radius). The function of the brake causes changes in braking torques and other, mainly undesirable, effects in a very complex way. Nonetheless, attempts have been made on numerous occasions to explore these mechanical and thermal phenomena relating to the dynamic behaviour of the disc, pad, calliper, and other devices. (Ostermeyer & Müller, 2008)

Wear debris is created when the brake pad material is pressed on the brake disc. In theory, two scenarios are possible. First, only the soft matrix is in contact. This is solely the case for 'green' pads. Second, there is also contact between inhomogeneities and the disc (general case). Wear particles pass through the contact zone of the brake pad. When the wear particles reach the rim of the contact zone, a portion of them stick to the brake disc and travel back into the contact zone after one revolution of the disc. Another portion is released into the environment. When a SiO_2 particle or similar hard inhomogeneity reaches the surface of the brake pad due to wear of the polymeric matrix, two essential processes occur. First, the particle is forced into the polymeric matrix due to the increased wear rate of the polymeric matrix compared to the hard particle. Second, the flow of wear particles in the boundary layer is disrupted. The local temperature will rise as a result of the increased local normal and tangential stresses in the particle's surroundings (Ostermeyer & Müller, 2008).

2.2. Solid Lubricant.

For a long time, industries have used solid lubricating materials to achieve low friction and wear under varying conditions. Because of their unique structures and physicochemical properties, molybdenum disulfide (MoS_2), tungsten disulfide (WS_2),

hexagonal boron nitride (HBN), and borides (MgB_2 and ZnB_2) have been used as lubricant additives or as strongly bonded protective coatings deposited by advanced vacuum processes. These materials form a protective film to keep friction pairs apart for improved friction reduction and wear resistance performance. (Mitchell, 1984). Because of their low shear strength, some soft metals, such as Cu, Ag, Sn, and Au, are used on sliding surfaces as lubricant additives or as soft metallic films to provide low friction coefficients. (Zhou et al., 1999)& (Verma et al., 2012). However, when compared to other solid lubricants, carbon has sparked the most interest due to its exceptional properties. Carbon exists in a variety of forms, and the properties of each form are determined by its unique structure. (Lettington, 1998). These various carbon forms have been studied for decades without exhausting their wonders and challenges.

2.2.1. Diamond like carbon

Due to their outstanding physical, mechanical, biomedical, and tribological properties, diamond-like carbon films are the most promising carbon-based protective coatings. (Cui et al., 2014). Significant progress has been made in the development and understanding of DLC in recent years, allowing it to become one of the most promising engineering materials for a variety of industrial applications such as manufacturing, transportation, microelectronics, and biomedical fields (Bewilogua & Hofmann, 2014). (Hauert, 2004) reviewed the industrial and medical applications of DLC coatings, taking into account their low friction coefficient, high wear resistance, and biological inertness, and also discussed the friction mechanism concerning the so-called transfer layer under various experimental setups and lubrication conditions, whereas (Donnet & Grill, 1997) presented an overview of the biomedical characteristics. Finally, (Kalin et al., 2008) investigated the

boundary lubrication behaviour of DLC/DLC and doped-DLC/doped-DLC contacts lubricated by oils with extreme-pressure (EP) and anti-wear (AW) additives and concluded that DLC/DLC contacts had the lowest friction with oils and the highest friction using oil with an EP additive, and also concluded that the hydrogen content in DLC coatings plays a crucial role in the tribological performance under lubricated and non-lubricated conditions.

(Donnet, 1996) compared the friction behaviour of two types of solid lubricants (pure MoS₂ and hydrogenated DLC) from a pressure range of less than 5×10^8 hPa to atmospheric air pressure and discovered that the friction coefficient of DLC increases from less than 0.01 to 0.15 as the pressure increases from ultrahigh vacuum to humid ambient air. This suggests that DLC could be a viable candidate for use as a novel solid lubricant in space applications. Maintaining reliable and accurate operation in low earth orbit (LEO) or inner space is a challenge for artificial satellites and spacecrafts equipped with various moving mechanical assemblies (Takano, 1999). The tribology technique has been a key factor in space exploration, particularly the effects of space environments on lubricating materials, due to the continuous improvement of machine elements over the last few decades. The space environment is vastly different from that of Earth, with a high vacuum, temperatures that fluctuate between -120 and 150 °C due to the influence of sunlight, and harsh space irradiation.

Direct contact between metallic surfaces in such harsh environments would result in high friction and wear due to seizure or even cold welding, which could easily inflict fatal damage on satellites and spacecrafts with no possibility of repair. Protective coatings are critical because they can keep moving surfaces from making direct contact. As a result, studying the physical and tribological properties of DLC films under space environments such as high vacuum, fluctuating temperatures, and irradiation is a prerequisite for space

applications of DLC as protective coatings (Enke et al., 1980) first reported low friction coefficients (0.01–0.02) of DLC films under vacuum as early as 1980.

2.2.2. Graphite.

Graphite has long been used in industry as a typical 3D solid lubricant. Graphite is said to be more lubricious in humid environments than in dry or vacuum environments (Bryant et al., 1964). Water molecules can penetrate the space between graphite layers in a humid environment, making graphite easy shearing and low friction. Furthermore, graphite scrolls can be formed during the tribological process to reduce surface energy and thus friction in sliding interfaces (Berman et al., 2014). (Berman et al., 2014) compared the tribological properties of graphite to their previous research on graphene [(Berman et al., 2013a) & (Berman et al., 2013b, 2014)]. Graphite and graphene tribological tests were performed under the same test conditions in humid air and dry nitrogen. Their findings revealed that graphite powder had high friction and wear losses in a dry nitrogen environment, whereas graphene wear was significantly reduced in both humid air and dry nitrogen environments (Figure 2-8).

Graphite has also been mixed with metals to create composite coatings. (Chen et al., 2018) prepared Cu-Al₂O₃-graphite solid-lubricating coatings by incorporating Cu-coated graphite into Cu-10 wt percent Al₂O₃ spray powder. When compared to pure graphite, the coatings' superior tribological performance was enabled by the stable adhesion between Cu-coated graphite and Cu powder. The composite coating had a relatively low friction coefficient due to the combined effect of hard reinforcement (Al₂O₃) and solid lubricant (graphite) (0.29).

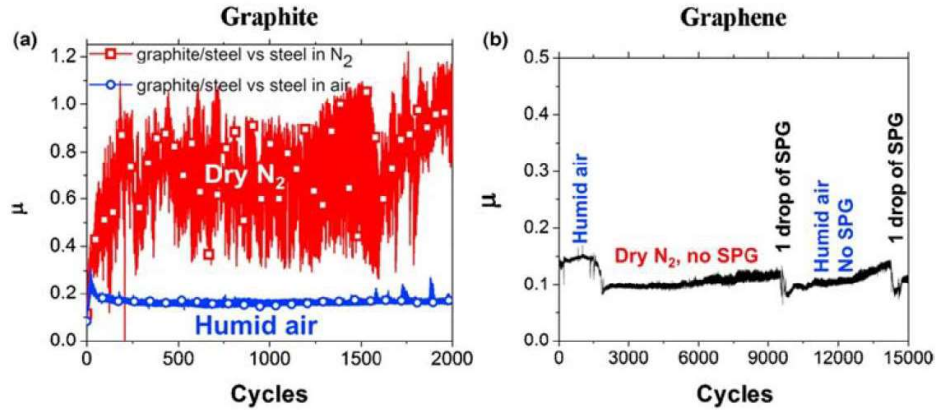


Figure 2-8: Coefficient of friction of graphite (a) and graphene (b) in different atmospheres.

(Berman et al., 2014)

2.3. Palm Kernel Activated Carbon

Many studies have been conducted to reduce wear and friction in tribological applications by investigating various types of lubricants or coating materials. Several researchers have discovered that composites activated by graphite or carbon have the potential to act as self-lubricating materials when reinforced with other metals such as aluminium. (Li et al., 2011). Natural polymer composites are a more environmentally friendly version of polymer composites because they are reinforced with natural elements like corn fibre, kenaf powder, and palm ash rather than synthetic fibres like glass and carbon fibres. (Mat Tahir et al., 2016). In order to meet the global demand for lightweight, high performance, eco-friendly, wear and corrosion resistant materials, a significant amount of research has recently shifted focus from monolithic materials to composite materials. The benefits of composite materials include their permeability, low cost, and various strengthening mechanisms. (Rymuza, 2007) & (Uvaraja et al., 2013).

PKAC (Palm Kernel Activated Carbon) is a by-product of the palm oil extraction process. This waste contains carbon properties as well as residual oils (natural lubricants), and it has the potential to become a new self-lubricating material. The cost of current commercial self-lubricating material is relatively high. Thus, incorporating a carbon material derived from agricultural wastes as new reinforcement substitutes in the fabrication of polymer matrix composites is thought to have a high potential for a zero-waste strategy for improving tribological properties at a low cost. (Bakry et al., 2013)

Polymer materials, in general, have poor physical-mechanical properties when compared to metals or ceramic materials. As a result, natural fillers (fibres, particles, or powders) derived from plant sources are used to reinforce polymer resins. (Shuhimi et al., 2016). To meet high strength/high modulus requirements, activated carbon particles can be used to modify the properties. (La Mantia & Morreale, 2011). These composite materials are also prone to failure due to mechanical damage caused by tension, flexural, and compression forces. As a result, using materials with higher damage tolerance and adequate mechanical evaluation is critical to reducing problems. (Banakar et al., 2012). Cracking, low toughness, and low tensile strength have resulted in poor durability, which has resulted in increased composite material maintenance costs. (Yang et al., 2017). The composition of engineering materials and surface modification have made significant contributions to the improvement of mechanical properties. composite performance (Abdullah et al., 2011). Most engineering composite materials requiring carbon reinforcement in thermosetting epoxy polymer have seen a significant improvement in recent years. (Banakar et al., 2012).

Furthermore, epoxy resin is commonly used as a thermoset material in polymeric composites because it has good chemical and insulation properties, as well as good bonding strength with other materials. (Uygunoglu et al., 2015). According to some researchers,

combining graphite or carbon with other materials has a high potential for producing composites that reduce wear and friction. The production of activated carbon from palm kernel with high porosity as reinforcement in a polymer matrix to function as a self-lubricating material has been tested by (Chua et al., 2014) and is available at affordable costs. Because of its low friction coefficient value, palm kernel activated carbon reinforced polymeric composite has the potential to replace the current high-cost commercial self-lubricated material.(Mat Tahir et al., 2016).

2.3.1. Physical properties PKAC.

From previous study about physical and mechanical properties of PKAC, they are comparing those properties by different percentage of composition PKAC and epoxy. Hardness values at room temperature increased from 89.5 (75-25 percent sample) to 95.1 (70-30 percent sample) and then increased until they reached a maximum of 96. (65-35 percent sample). Meanwhile, a slight difference in hardness values was obtained, despite the fact that the hardness test was performed at 90°C using the same procedures. At 90°C, the hardness values increased from 86.3 (75-25 percent sample) to 93.1 (70-30 percent sample), and then to a maximum of 94. (65-35 percent sample). The average hardness values of palm kernel activated carbon reinforced polymeric composites demonstrated that the hardness of the composites began to decrease from room temperature to 90°C(Mohmad et al., 2018). This finding was supported by a study conducted by (Brostow et al., 2010), which discovered that temperature had a direct impact on polymeric composites. Material hardness decreased as temperature increased, which was also consistent with the previous study by (Nayani et al., 2013). The reason for these phenomena is that a higher molecular mass results in a harder final cured material. (Goud & Rao, 2012) discovered that increasing the glass fibre molecular

mass resulted in a significant increase in the tensile, flexural, impact, and hardness properties of glass fibre hybrid composites.

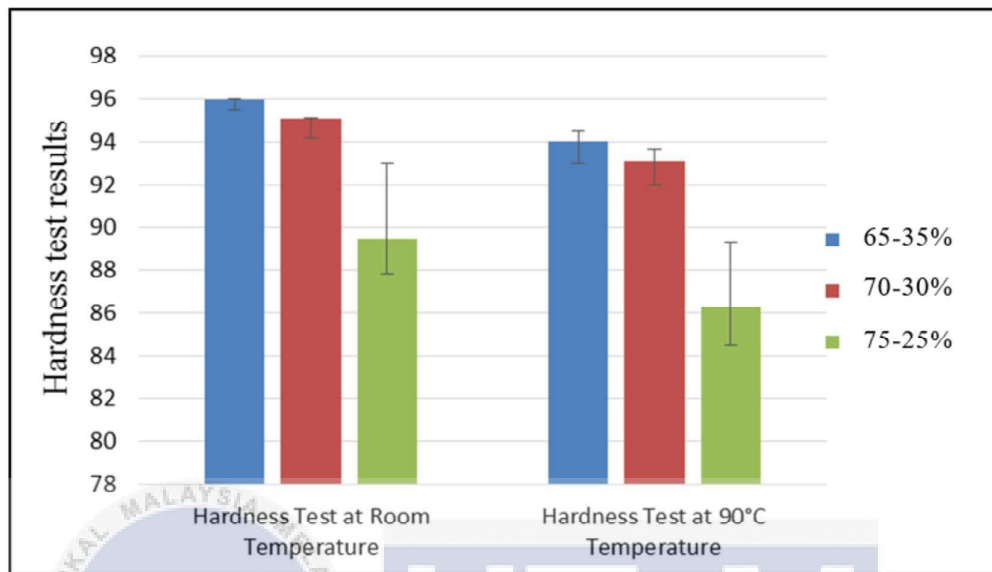


Figure 2-9: Hardness of palm kernel activated carbon reinforced polymeric composite at room temperature and at 90°C. (Mohmad et al., 2018)

The adhesion and density of epoxy resin in the polymeric composites influenced the reinforcement of this activated carbon. Indeed, increasing the carbon concentration influenced the wettability of the particles with the epoxy resin. The density test results of the composite with different ratios of palm kernel activated carbon mixed with polymer epoxy are shown in Figure 2-10. The addition of an epoxy matrix increased the density to a certain carbon content ratio, which was 70%, and then the density began to decrease after this ratio of carbon content due to the low interfacial bonding between carbon particles and epoxy at 75% composition. The addition of 70% carbon resulted in high adhesion forces between the composite's molecules. The reason for this was to improve the interfacial bonding with

epoxy and to reduce micro-voids by increasing the density of this composite. As a result, the density decreased while increasing the carbon content up to 70%, demonstrating that higher density could be obtained by combining 70% carbon with 30% epoxy. As a result, the density decreased while increasing the carbon content up to 70%, demonstrating that higher density could be obtained by combining 70% carbon with 30% epoxy (Mohmad et al., 2018).

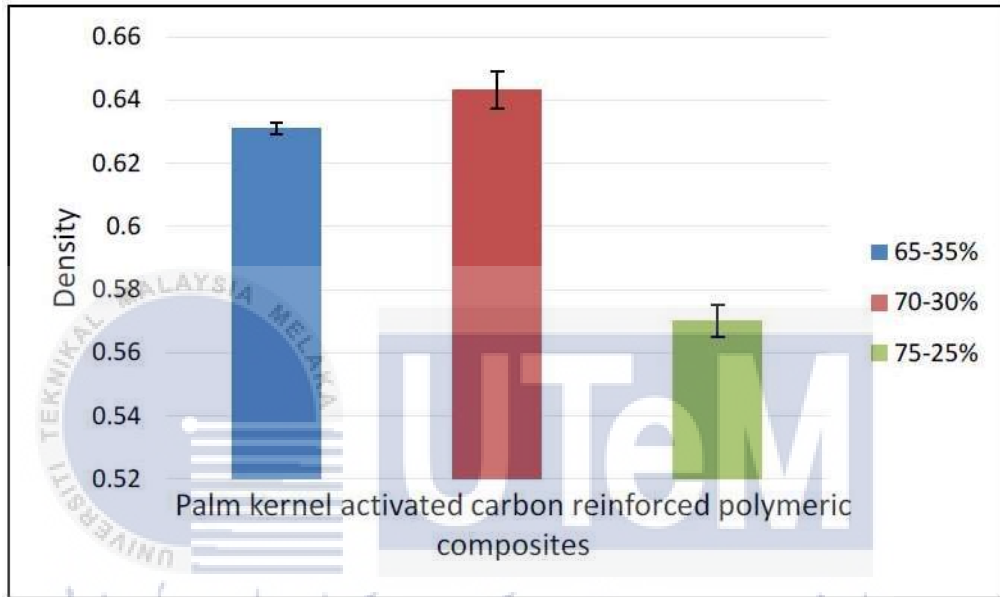


Figure 2-10: Density of palm kernel activated carbon reinforced polymeric composite at different compositions. (Mohmad et al., 2018)

This composite was found to have a high degree of porosity (14.6 percent) calculated in the surface area (75-25 percent). Meanwhile, the (65-35 percent) sample had the lowest porosity (10.7 percent),s confirming that the internal bonding between the particles and the epoxy was the best compared to the other two composites. The sample's good interfacial bonding (65-35 percent) meant that there were fewer voids, which allowed water to enter the

samples. Water molecules could enter the structure of a polymeric composite if the porosity of the composite increased.

The porosity ratio varied for each composition of palm kernel activated carbon reinforced polymeric composite. The increasing rate of porosity was largely related to the reinforcement content for each of them, implying that porosity increased proportionally with the amount of activated carbon in the composite until reaching the highest level with the 75-25 percent composite. This was due to the saturation state of carbon with the epoxy resin and the formation of bonds between them. The absence of epoxy resulted in the formation of undesirable voids in the composite (Mohmad et al., 2018).

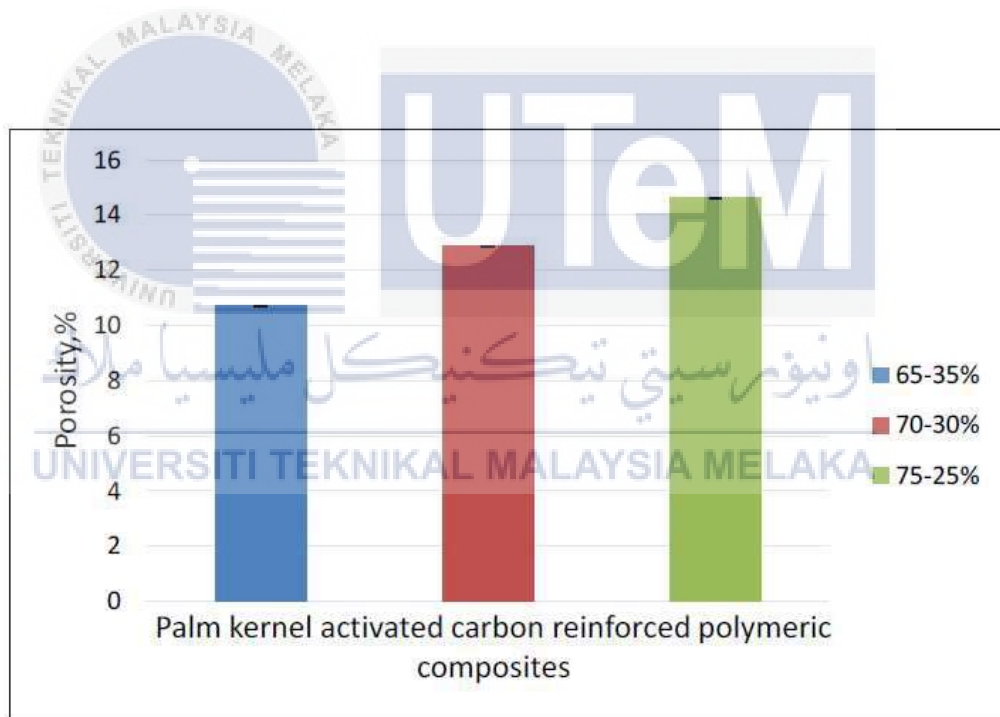


Figure 2-11: Porosity of palm kernel activated carbon reinforced polymeric composite at different compositions. (Mohmad et al., 2018)

2.3.2. Mechanical properties of PKAC

The tensile test results are shown in Figures 2-12 and 2-13. The elastic modulus of the various compositions has been determined using the tensile test. Figure 2-12 shows that increasing the percentage of activated carbon from 65 to 70% resulted in stronger bonding. According to (Arash et al., 2015), the weight percentage or ratio of a composite can increase its elastic modulus. Unfortunately, after adding another 5% of activated carbon, the value of elastic modulus immediately decreased. This could be attributed to the particles' weak interfacial bonding. According to (Uygunoglu et al., 2015), the interfacial adhesive bond has the greatest influence on elastic modulus. Aside from that, it could have been caused by the high distribution of voids caused by the low amounts of epoxy resin used to hold the activated carbon particle.

Figure 2-13 depicts the ultimate tensile stresses of composites with different proportions of palm kernel activated carbon (65%, 70%, and 75%) to polymer epoxy. Figure 2-13 shows that there was little difference between ultimate tensile stress values of 65-35 percent and 70-30 percent. However, there was a significant difference in the ultimate tensile stress value with a proportion of 75% activated carbon, owing to poor dispersion and weak bonding of the carbon with the resin matrix of this composite. Because some of the specimens from the 75 percent group failed in the elasticity region, the 75 percent samples appeared to be more brittle. Although the ultimate tensile strength of 75% was not significantly different from that of 65%, the composition of 70% could withstand the maximum load of 1306N, which was the highest load among the compositions (Mohmad et al., 2018).

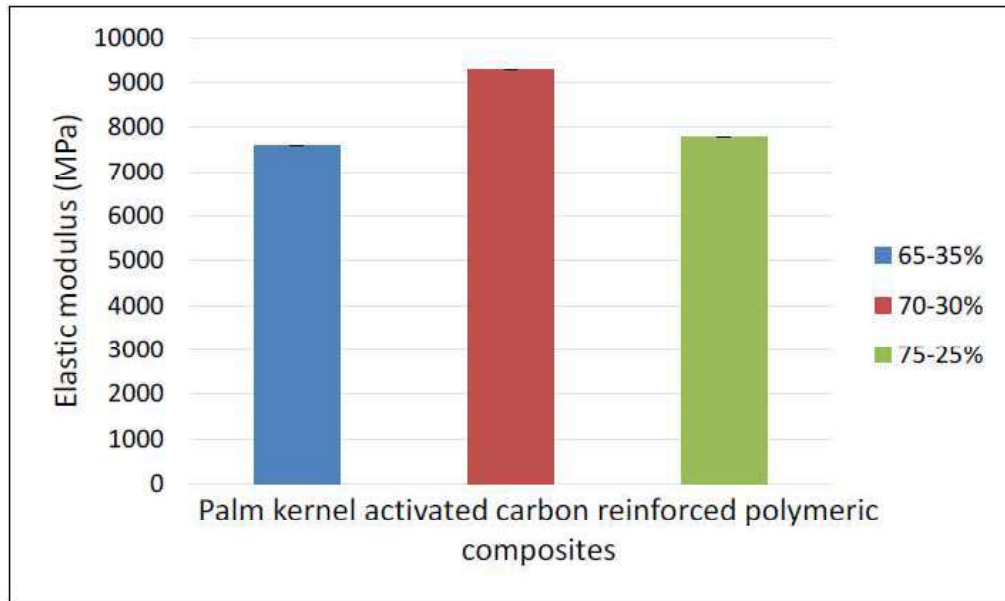


Figure 2-12: Average elastic modulus of palm kernel activated carbon reinforced polymeric. (Mohmad et al., 2018)

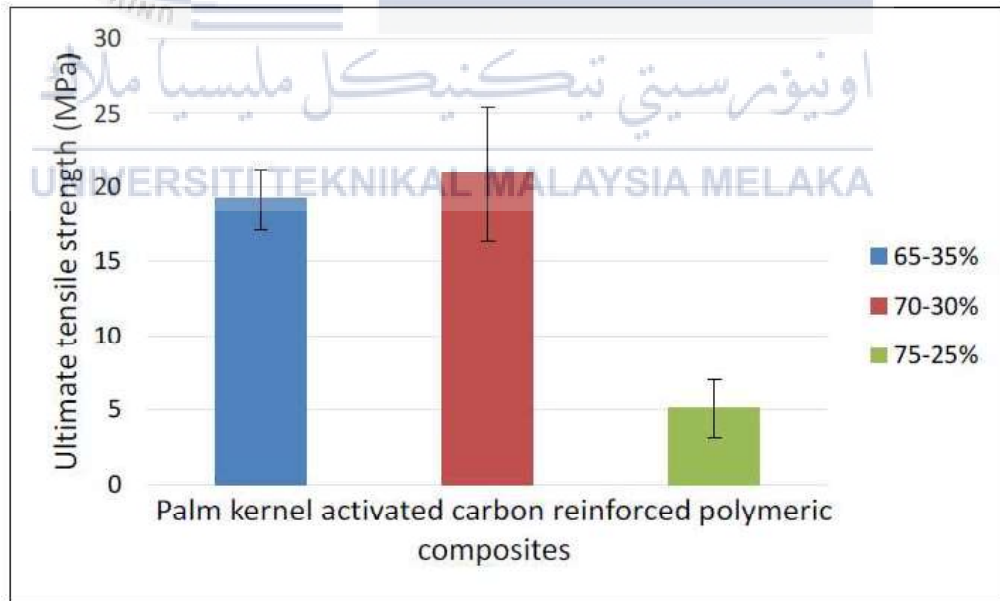


Figure 2-13: Average ultimate tensile strength of palm kernel activated carbon reinforced polymeric. (Mohmad et al., 2018)

2.4. Vegetables oils.

Vegetable oils are glycerides of fatty acids that are liquid or semisolid plant products. Figure 2-14 depicts a triglyceride's schematic structure. In comparison to mineral oils, the chemical structure of vegetable oils is relatively homogeneous. The composition of vegetable oil is determined by the "fatty acids," which are plant-specific building blocks. Triglycerides are formed when fatty acids form an ester bond with glycerol. Only the cis structure of fatty acids is found in nature. With regard to the region, environmental circumstances, and availability of resources for growth, there is a possibility of difference in the fatty acid proportion for a given oil. The fatty acids are composed of straight chain carbon molecules ranging from 8 to 24 carbon atoms. A brief note on different kinds of fatty acids is presented in the following section. (Reeves et al., 2012)

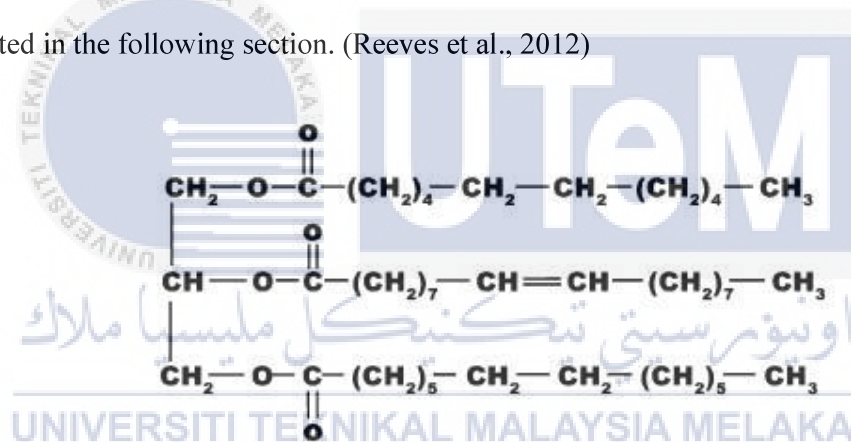


Figure 2-14: Schematic representation of a triglyceride molecule.

- a. Saturated fatty acids are fatty acids that lack a carbon–carbon double bond in their backbone structure, such as Lauric acid, Palmitic acid, and Stearic acid. They have a high pour point and are resistant to oxidation. Figure 2-15 shows a schematic illustration of a saturated fatty acid.(Reeves et al., 2012)

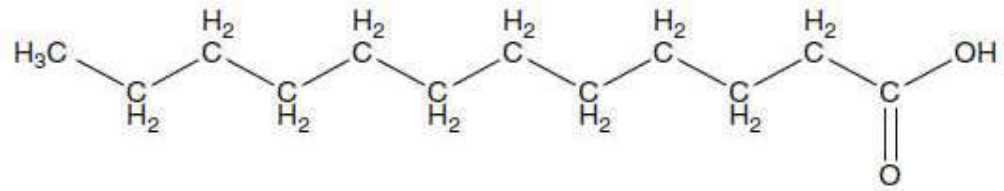


Figure 2-15: Schematic representation of a saturated fatty acid.

b. Monounsaturated fatty acid: Monounsaturated fatty acids are those that have only one carbon–carbon double bond in their backbone structure, such as Oleic acid. They have a low pour point and provide a reactive site (or sites) for chemical modification.(Reeves et al., 2012)

c. Polyunsaturated fatty acids, such as Linoleic and Linolenic acids, are fatty acids with more than one carbon–carbon double bond in their backbone structure. They have a low pour point and provide a reactive site for chemical modification, yet they are extremely vulnerable to oxidation. Figure 2-16 a and b illustrate a schematic illustration of monounsaturated and polyunsaturated fatty acid structures, respectively.(Reeves et al., 2012)

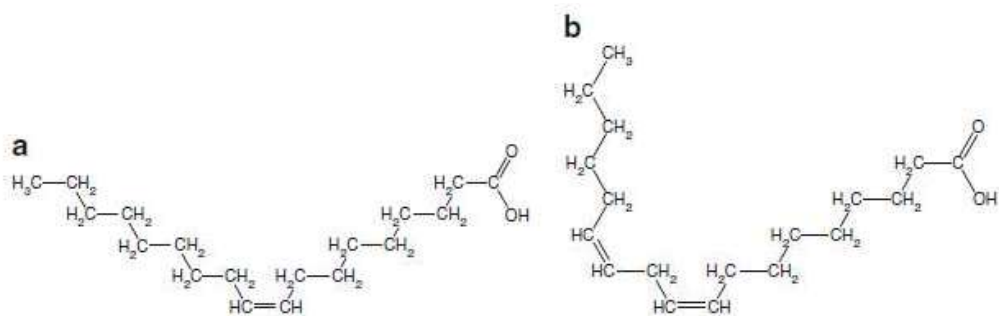


Figure 2-16: Schematic representation of (a) monounsaturated and (b) polyunsaturated fatty acids

- d. Hydroxy fatty acids are fatty acids with one hydroxyl group (OH) in their backbone structure, such as Ricinolein acid in Castor oil. They have a low pour point and many reactive sites for chemical modification due to the presence of hydroxyl groups. Figure 2-17 shows a schematic illustration of a hydroxyl fatty acid.(Reeves et al., 2012)

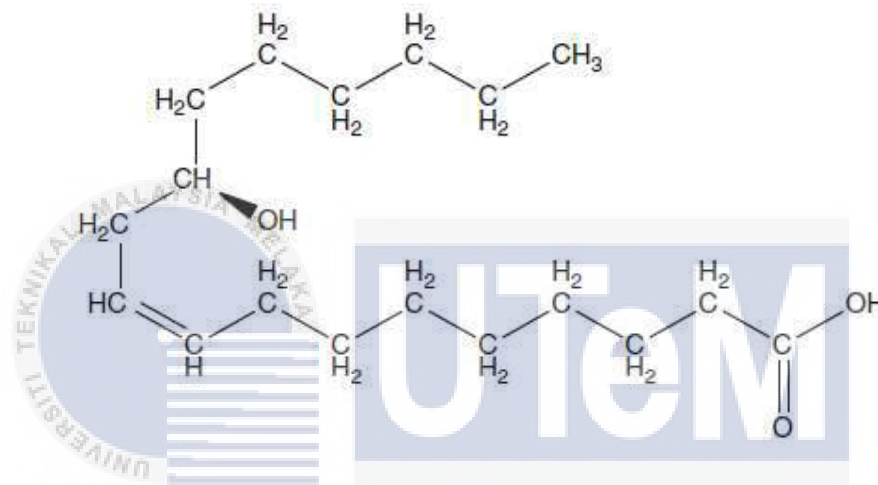


Figure 2-17: Schematic representation of a hydroxy fatty acid.

- e. Fatty Acids: This is a special fatty acid found in Vernonia seed oil that kills helminths and a fatty acid called vernolic acid. A representative diagram of an epoxy fatty acid is shown in Fig. 2-18.(Reeves et al., 2012)

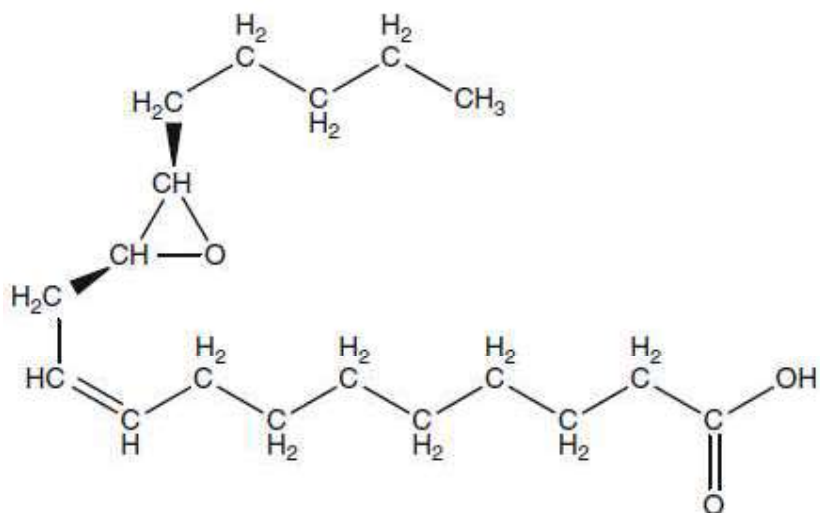


Figure 2-18: Schematic representation of an Epoxy fatty acid.

2.4.1. Tribology and Applications of Vegetable Oils

In essence, the triglyceride structure of vegetable oils provides many desirable qualities for lubricants. Fatty acid chain length plays a very important role in controlling wear rate and coefficient of friction. The presence of a long polar fatty acid adsorption surface film resists the penetration of irregularities and suppresses metal-to-metal contact, thereby reducing friction and wear. Strong intramolecular interactions between fatty acid molecules are also responsible for the high viscosity index observed in vegetable oils. (Menezes et al., 2013)

Attempts were made to evaluate the bioavailability of green liquid lubricants using a pin on disk device (Reeves et al., 2012). In particular, various green liquid lubricants such as avocado, canola (rapeseed), corn, olives, peanuts, safflower, sesame seeds, and vegetable oils are possible. Figure 2-19 shows the changes in friction and wear rate of these lubricants. Avocado oil has been found to offer the best friction and wear performance compared to

other green lubricants. We conclude that high levels of monounsaturated fatty acids present in oils, especially natural oils containing oleic acid, develop densely packed carbon chains that better protect the interface between pins and discs, reducing friction and wear. It was attached (Menezes et al., 2013).

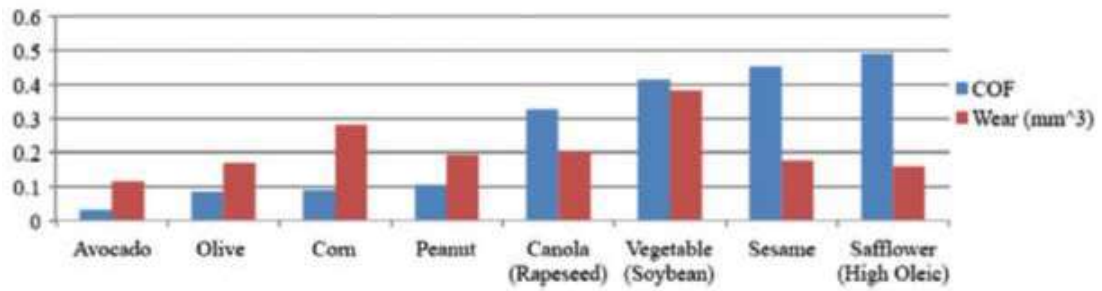


Figure 2-19: Variation of coefficient of friction and wear rate for vegetable oils. (Reeves et al., 2012)



CHAPTER 3

METHODOLOGY

3.0. Introduction.

The objective of this study is to investigate the effect on physical and mechanical properties of palm kernel activated carbon after immersion in different type of vegetables oil. This chapter will describe the method used in this project to get the desired results. Overall operational flow is to illustrate the order to conduct the experiment as shown in Figure 3-1.

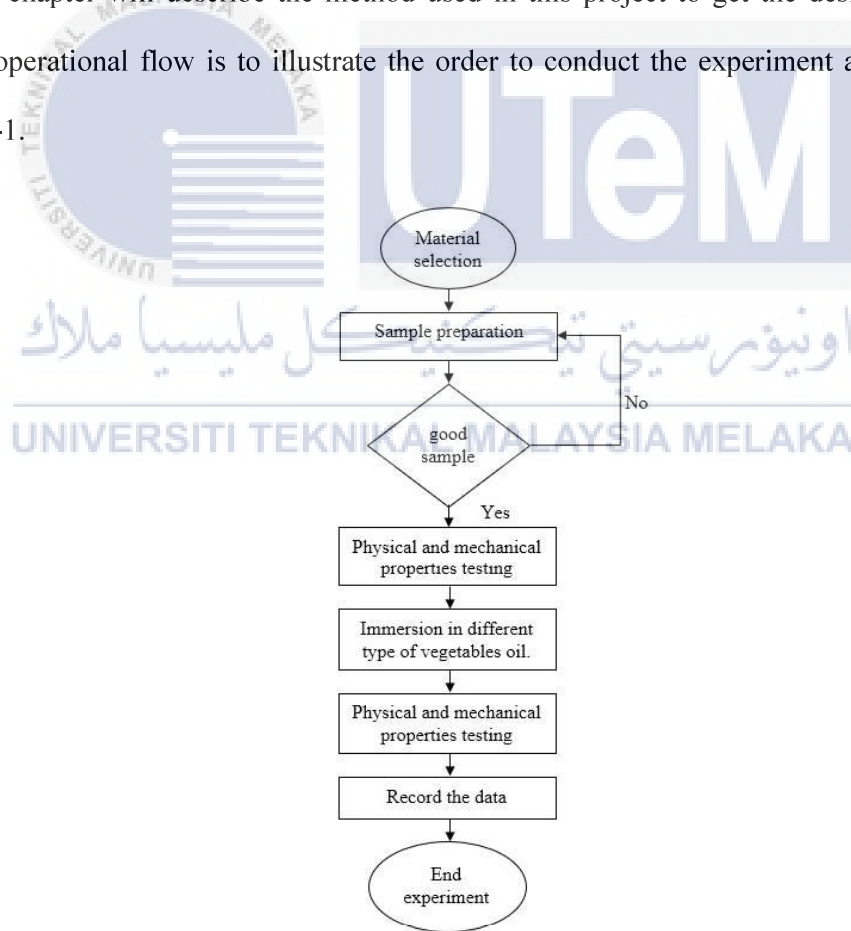


Figure 3-1: Flow Chart for Experiment.

3.1. Sample preparation.

The material used to make sample is palm kernel activated carbon (PKAC) from wastes of agriculture activities. West system 105 Epoxy resin and West System 206 slow Hardener was provided by Universiti Teknikal Malaysia Melaka which is to mix with PKAC to prepare the sample.



Figure 3-2: Palm Kernel Activated Carbon (PKAC).
اونيوور تي تي تيكيكلاي املاك



Figure 3-3: West System 105 Epoxy Resin.



Figure 3-4: West System 206 Slow Hardener.

The raw material of PKAC were crushed in the crusher to make it fine. Then, the crushed PKAC were transferred into the sieving machine for about 10 minutes to filter the crushed PKAC into several fine sizes such as 300, 250 and 63 μ m. The process had to be done several times to get adequate powder to be used in preparing the sample.



Figure 3-5: Crusher machine.



Figure 3-6: Sieving machine.

Disc, pin and bone shape of sample need to prepare to run physical and mechanical test. Disc shape used to run physical properties testing such as hardness, surface roughness, density, water absorption and porosity. For mechanical properties testing, pin shape used in compression test and bone shape used to conduct tensile test. The 250 μ m in size of PKAC powder have been selected to be mix with a binder known as high-density epoxy [West system 105 epoxy resin (Figure 3-2) and West system 206 slow hardener (Figure 3-3)]. 70%, 65% and 60% of PKAC are prepared to complete this research. The dimension for disc shape is 74mm diameter and 5mm thickness. For pin shape, the length is 3cm and diameter 1cm. For bone shape, the length 16.4cm and 2mm thickness. The mixture then inserted to mould and going through heating process at the same time being compress for about 10 minutes with 100°C of hot press machine plate and 120kPa. The sample then going through curing process for about 7 days before proceeding to test.



Figure 3-7: 250 μ m in size of PKAC.



Figure 3-8: Mould for Disc shape.



Figure 3-9: Mould for bone shape.

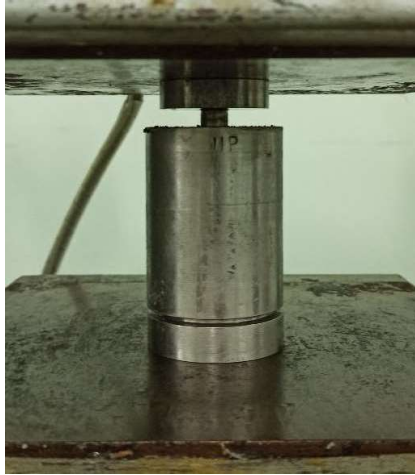


Figure 3-10: Mould for pin shape.

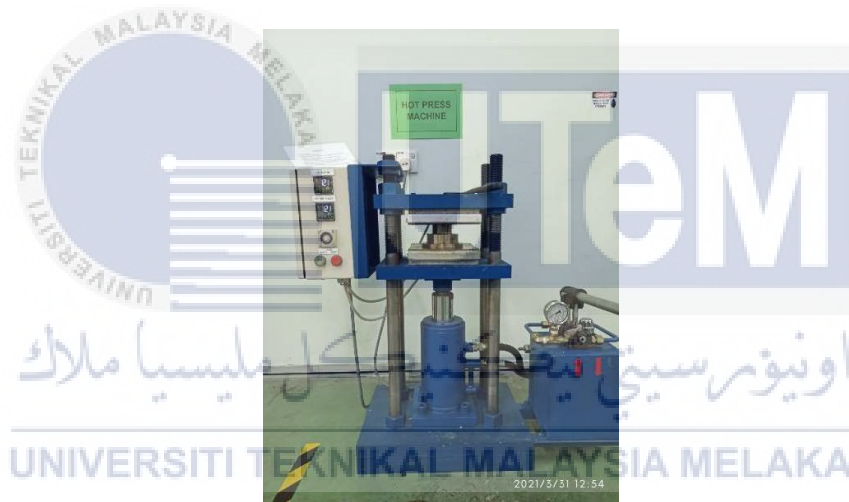


Figure 3-11: Hot press machine.

Table 3-1: Amount of PKAC and Epoxy for disc shape sample.

Disc				
Palm Kernel Activated Carbon		Epoxy (Resin to hardener ratio of 4:1)		
Composition (%)	Weight of PKAC (g)	Composition (%)	Weight of Epoxy (g)	Weight of Hardener (g)
60	17.16	40	9.16	2.28
65	18.59	35	8.00	2.00
70	20.2	30	6.86	1.72

Table 3-2: Amount of PKAC and Epoxy for pin shape sample.

Pin				
Palm Kernel Activated Carbon		Epoxy (Resin to hardener ratio of 4:1)		
Composition (%)	Weight of PKAC (g)	Composition (%)	Weight of Epoxy (g)	Weight of Hardener (g)
60	2.15	40	1.07	0.36
65	2.33	35	0.94	0.31
70	2.51	30	0.81	0.27

Table 3-3: Amount of PKAC and Epoxy for bone shape sample.

Bone				
Palm Kernel Activated Carbon		Epoxy (Resin to hardener ratio of 4:1)		
Composition (%)	Weight of PKAC (g)	Composition (%)	Weight of Epoxy (g)	Weight of Hardener (g)
60	8.58	40	4.58	1.14
65	9.30	35	4.00	1.00
70	10.10	30	3.43	0.86



3.2. Physical properties test.

After complete preparing the sample, then it is weighted by using weight scale with ability measure until 0.0001g. The hardness of the sample was measured using Shore Hardness Durometer-D. By applying a force on the standardized presser foot, it will penetrate into the material and the indentation depth is measured by the durometer. Greater numbers on the scale indicate the materials are hard while lower numbers indicate the materials are soft. Then, the roughness tester is used to determine the surface roughness of the sample.



Figure 3-12: Weight scale.



Figure 3-13: Shore Hardness Durometer-D.



Figure 3-14: Surface roughness tester profilometer.

For density test, the sample density determined by measuring each of specific gravity and the total volume of the samples using an electronic densitometer. The electronic Densimeter gives very precise calculations on the specific gravity of an object of any shape. For porosity, the sample need to immerse in vegetables oil and weight it then the mass after immersing minus mass before immerse divide with mass after immersing.

$$Porosity = \frac{m_{after} - m_{before}}{m_{after}} \times 100$$



Figure 3-15: Electronic densitometer.

Water absorption properties of palm kernel activated carbon reinforced polymeric composites had been analysed according to the ASTM D570 standard. The electronic balance with capable of reading to an accuracy of 0.0001g used to measure the sample initial

weight. Samples then immersed in water at room temperature of $23 \pm 1^\circ\text{C}$ for about 24 hours. Then the samples wiped off with a dry tissue and measured the final weight of the samples.

3.3. Mechanical properties.

The ASTM D3039 / D3039M-17 standard is typically used to perform tensile tests on polymeric composite samples with the speed of 2mm/min. The tensile strength, Young's modulus, and strain of a palm kernel activated carbon reinforced polymeric composite were determined in this test. The ASTM D6441 standard used to perform compression test on polymer matrix composites samples with the speed of 2.5mm/min. The compressive strength, Young's modulus, and strain of a palm kernel activated carbon reinforced polymeric composite were determined in this test. To accomplish this, an Instron universal testing machine with a capacity of 250 kN, a speed range of 0.001-500 mm/min, a test area of 1256 mm x 575 mm, and controlled by Bluehill 3 software with reference to the above-mentioned standard was used. (Mohmad et al., 2018)



Figure 3-16: Instron universal testing machine.

3.4. Immersing in different type of vegetable oil.

The physical and mechanical properties test of PKAC need to be done before and after immersing in various type of vegetables oil. There are 3 types of vegetables oil used which is palm oil, corn oil and soybean oil. The duration of the sample immerse in vegetables oil is 24 hours or 1 day.



Figure 3-17: Palm oil.

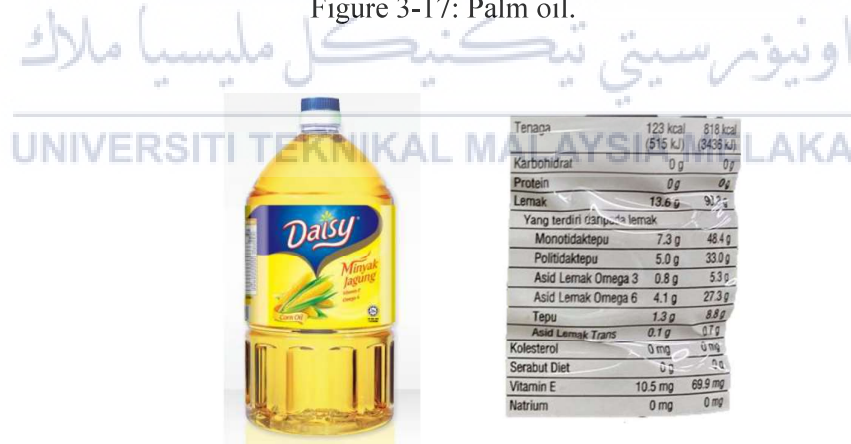


Figure 3-18: Corn oil.



NUTRITION INFORMATION	
(Serving per 100mg)	
Energy	3460 kJ
Protein	0 g
Total Fat	90.8 g
- Saturated Fat (Max)	27.9 g
- Monounsaturated Fat (Min)	33.8 g
- Polyunsaturated Fat (Min)	29.1 g
- Trans Fat (Max)	0 g
Cholesterol	0 g
Carbohydrate	0 g
Sugar	0 g
Sodium	0 g
Other	0 g
Cloud Point	BELOW 0°C

Figure 3-19: Soya oil.



CHAPTER 4

RESULTS AND DISCUSSION

4.0. Introduction

This chapter discusses the results obtained from the experiment which contains the hardness, surface roughness, density, water absorption, tensile and compression data. This includes data before and after immersing in different type of vegetables oil. This chapter is divided into eight sub-sections. Section 4.1 discuss on hardness, section 4.2 surface roughness, section 4.3 density, section 4.4 water absorption, section 4.5 porosity, section 4.6 tensile test and section 4.7 compression test.

4.1. Hardness.

The Shore D hardness test was conducted for all the specimens which is disc, pin and bone shape and the data obtained were tabulated as shown in figure below. It is consisted of different composition of PKAC and E-poxy and hardness before and after immersion in different type of vegetables oils.

Table 4-1: Hardness for disc before immersion in different type of vegetables oil.

	Sample No.	Hardness, HD			Average
60%	1	104.0	107.0	106.5	105.8
	2	105.0	106.5	104.5	105.3
	3	102.5	103.0	99.5	101.7
65%	1	103.0	104.0	106.0	104.3
	2	103.0	104.0	105.5	104.2
	3	103.0	105.5	104.0	104.2
70%	1	101.0	102.0	100.0	101.0
	2	101.5	101.5	100.5	101.2
	3	94.0	94.0	101.0	96.3

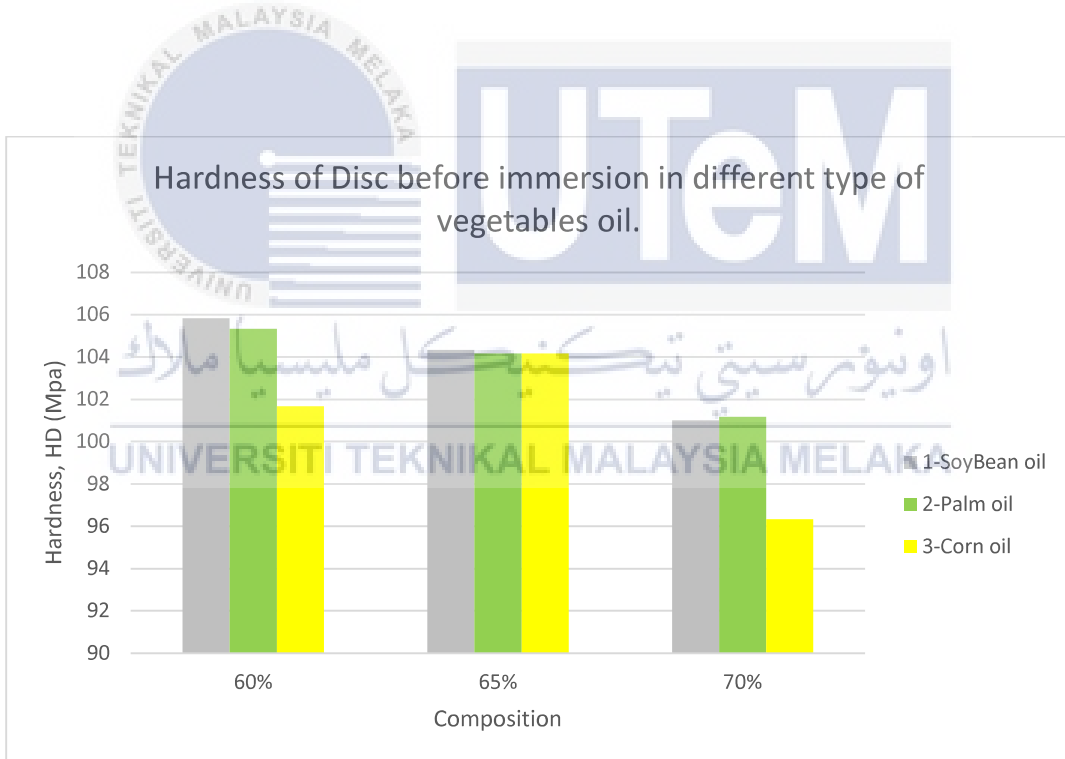


Figure 4-1: Hardness of disc before immersion in different type of vegetables oil.

Table 4-2: Hardness for disc after immersion in different type of vegetables oil.

	Sample No.	Hardness, HD			average
60%	1	104.0	106.5	106.5	105.7
	2	104.0	105.0	105.0	104.7
	3	104.0	102.0	104.0	103.3
65%	1	104.0	103.5	103.0	103.5
	2	104.0	105.5	104.0	104.5
	3	102.5	105.0	105.0	104.2
70%	1	99.0	102.5	103.0	101.5
	2	99.0	100.0	100.5	99.8
	3	94.5	94.0	97.0	95.2

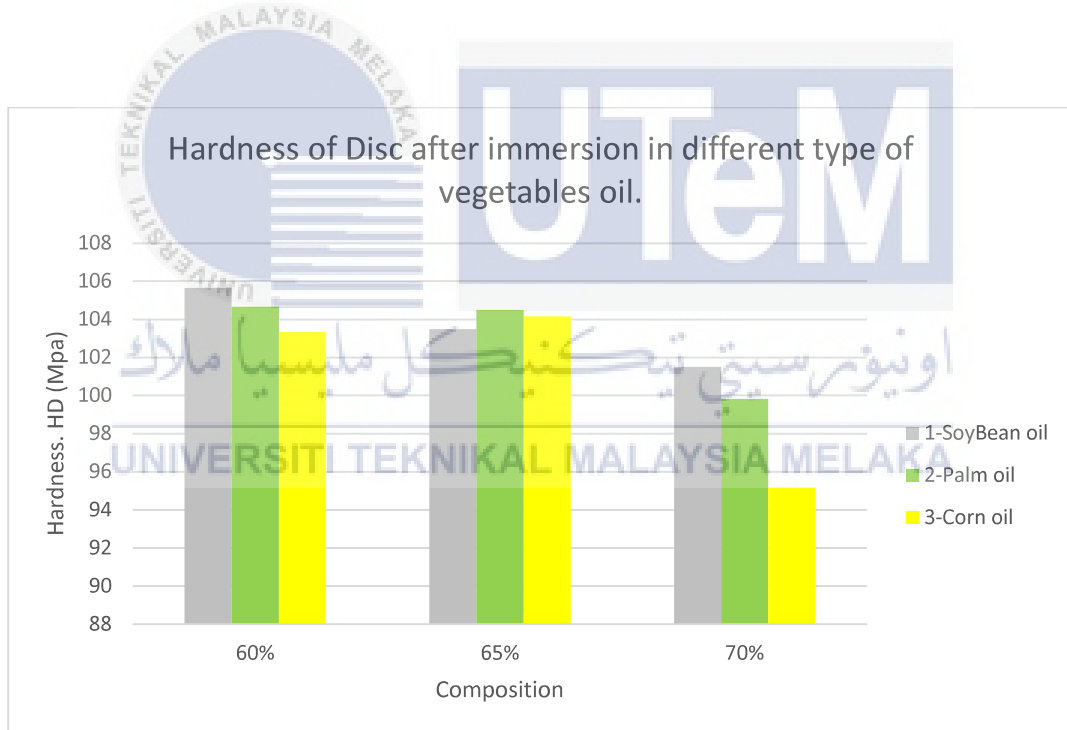


Figure 4-2: Hardness of Disc after immersion in different type of vegetables oil.

Based on figure 4-1, sample with composition of 60% of PKAC have higher hardness than other composition which is 65% and 70%. The average hardness for 60% is 105.1, 65% is 104 and 70% is 99.5. Comparison between before and after immersion in different type of

vegetables oil can obtained with figure 4-1 and figure 4-2. It shown slightly different in the hardness. Based on comparison of data obtained composition with 60% of PKAC for soybean and palm oil decrease but for corn oil increase. For 65% of PKAC, with soybean oil decrease, palm oil increase and corn oil remain unchanged. Lastly for 70% of PKAC, with soybean increase, palm, and corn oil both decrease in hardness.

The activation process between palm kernel activated carbon and epoxy in the composites occurred owing to the degradation of epoxy in the composite which decreased the hardness of the composite (Mohmad et al., 2018). From the data, it observed that the greater amount of epoxy in the composites produce high hardness value of the composite. As a result, the improved bonding strength between the carbon particles and the matrix was responsible for the increase in hardness. This is in accordance with the work of Nayani et al. (2013).

4.2. Surface roughness.

The surface roughness tester was used to obtain the surface roughness of disc sample and the data obtained were tabulated as shown in figure below. It is consisted of different composition of PKAC and E-poxy and surface roughness before and after immersion in different type of vegetables oils.

Table 4-3: Surface roughness for disc before immersion in different type of vegetables oil.

Composition	Sample No.	Surface Roughness, Ra			average
60%	1	2.626	2.681	2.715	2.674
	2	2.443	2.881	2.468	2.597
	3	2.997	2.949	3.503	3.150
65%	1	5.182	4.761	5.288	5.077
	2	3.823	4.081	4.289	4.064
	3	5.754	4.224	4.377	4.785
70%	1	5.927	5.994	5.646	5.856
	2	9.204	8.817	8.732	8.918
	3	7.365	6.481	6.697	6.848

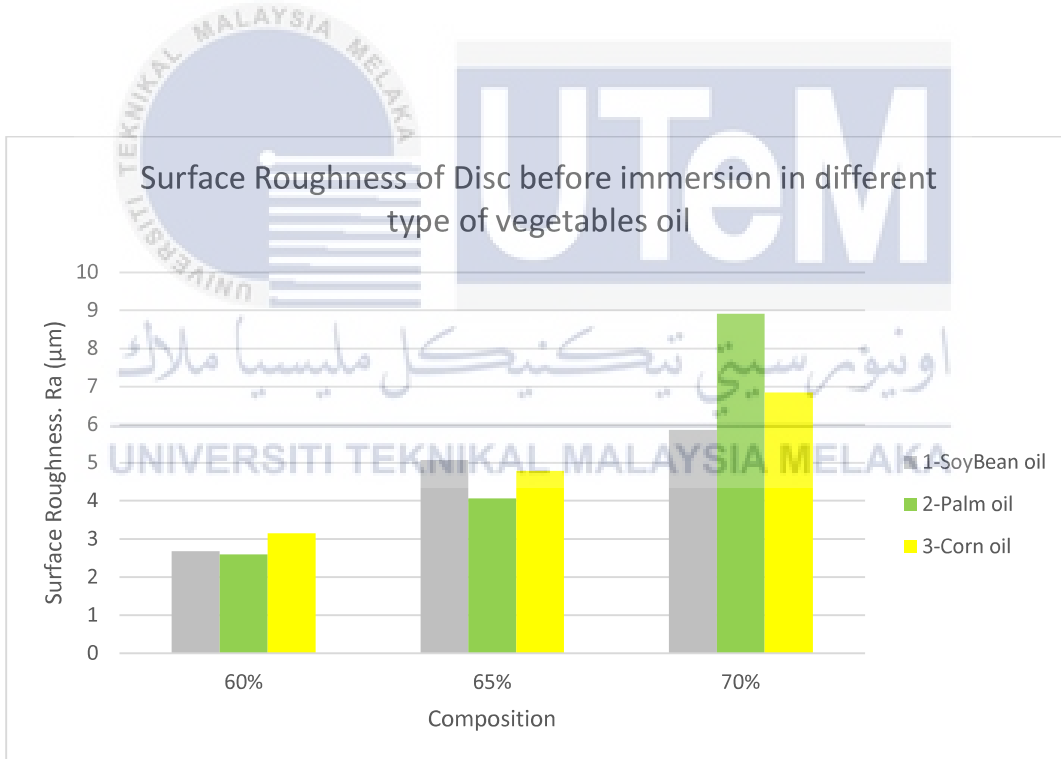


Figure 4-3: Surface roughness of disc before immersion in different type of vegetables oil.

Table 4-4: Surface roughness of disc after immersion in different type of vegetables oil.

Composition	Sample No.	Surface Roughness, Ra			average
60%	1	2.475	2.778	2.983	2.745
	2	2.109	2.271	2.041	2.140
	3	3.555	3.549	2.904	3.336
65%	1	6.309	5.963	5.509	5.927
	2	2.713	3.739	2.848	3.100
	3	6.955	4.632	4.004	5.197
70%	1	4.934	5.938	7.246	6.039
	2	6.081	6.327	6.246	6.218
	3	7.996	6.781	8.404	7.727

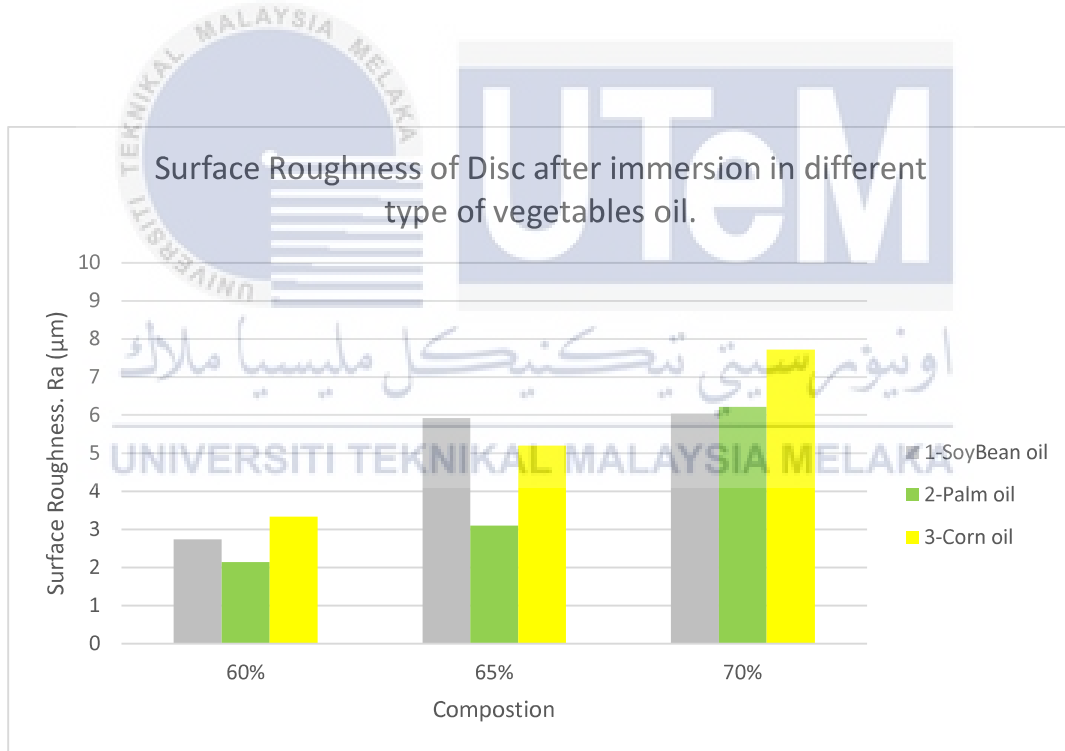


Figure 4-4: Surface roughness of disc after immersion in vegetables oil.

Based on table 4-3, sample with composition of 60% of PKAC have average surface roughness of $2.807\mu\text{m}$, for 65% has average surface roughness of $4.642\mu\text{m}$ and 70% has

average of $7.207\mu\text{m}$. Sample with 60% composition of PKAC have lowest average of surface roughness than 65% and 70% which means the lower the value indicates better surface roughness or smooth. Comparison between before and after immersion in different type of vegetables oil can obtained with table 4-3 and figure 4-4. For sample with composition of 60%, there are increasing value of surface roughness for soybean oil and corn oil but decreasing for palm oil. For sample 65% of PKAC, with soybean and corn oil there are increasing in value of surface roughness but decreasing with palm oil. For sample 70% of PKAC, both sample with soybean and corn oil increasing value but decreasing with palm oil.

The smoother the surface roughness, the smaller the coefficient of friction (Rahaman et al., 2015). Higher surface roughness with strong mechanical locking resistance contributed to the increased frictional force. This was the main reason why the coarser the surface, the higher the coefficient of friction. Due to the large surface roughness, most of the irregularities were deformed and worn due to high pressure and strong frictional shear. Proper surface roughness of the friction material helped to achieve high transmission efficiency. An ideal friction material with moderate roughness and low wear rate to ensure mechanical output stability and extend service life. (Song et al., 2019).

4.3. Density

The electronic densimeter was used to obtain the density of all the sample which is disc. The data obtained were tabulated as shown in figure below. It is consisted of different composition of PKAC and E-poxy and density before and after immersion in different type of vegetables oils.

Table 4-5: Density of disc before immersion in different type of vegetables oil.

Composition	Sample No.	Density, ρ			average
60%	1	1.331	1.332	1.332	1.332
	2	1.321	1.322	1.322	1.322
	3	1.228	1.228	1.228	1.228
65%	1	1.286	1.287	1.287	1.287
	2	1.322	1.323	1.322	1.322
	3	1.271	1.272	1.271	1.271
70%	1	1.211	1.212	1.212	1.212
	2	1.149	1.201	1.202	1.184
	3	1.226	1.231	1.239	1.232

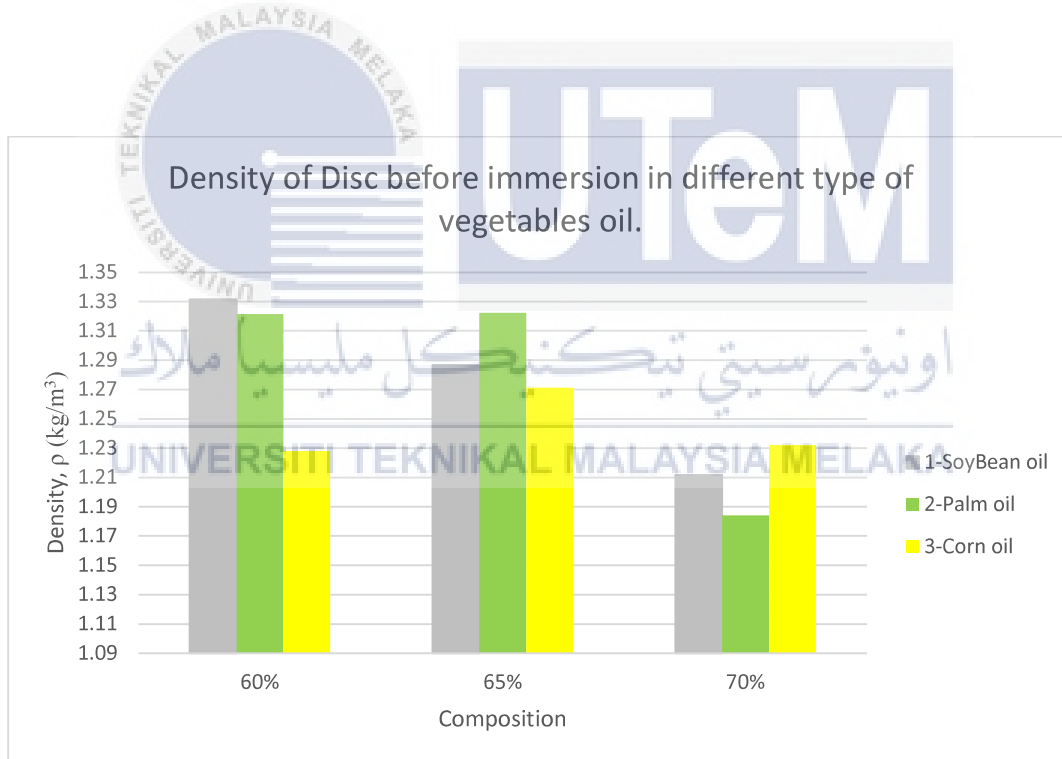


Figure 4-5: Density of disc before immersion in different type of vegetables oil.

Table 4-6: Density of disc after immersion in different type of vegetables oil.

Composition	Sample No.	Density, ρ			average
60%	1	1.337	1.336	1.337	1.337
	2	1.326	1.326	1.326	1.326
	3	1.247	1.247	1.248	1.247
65%	1	1.296	1.272	1.271	1.280
	2	1.326	1.327	1.326	1.326
	3	1.312	1.313	1.314	1.313
70%	1	1.269	1.272	1.271	1.271
	2	1.308	1.313	1.315	1.312
	3	1.277	1.277	1.277	1.277

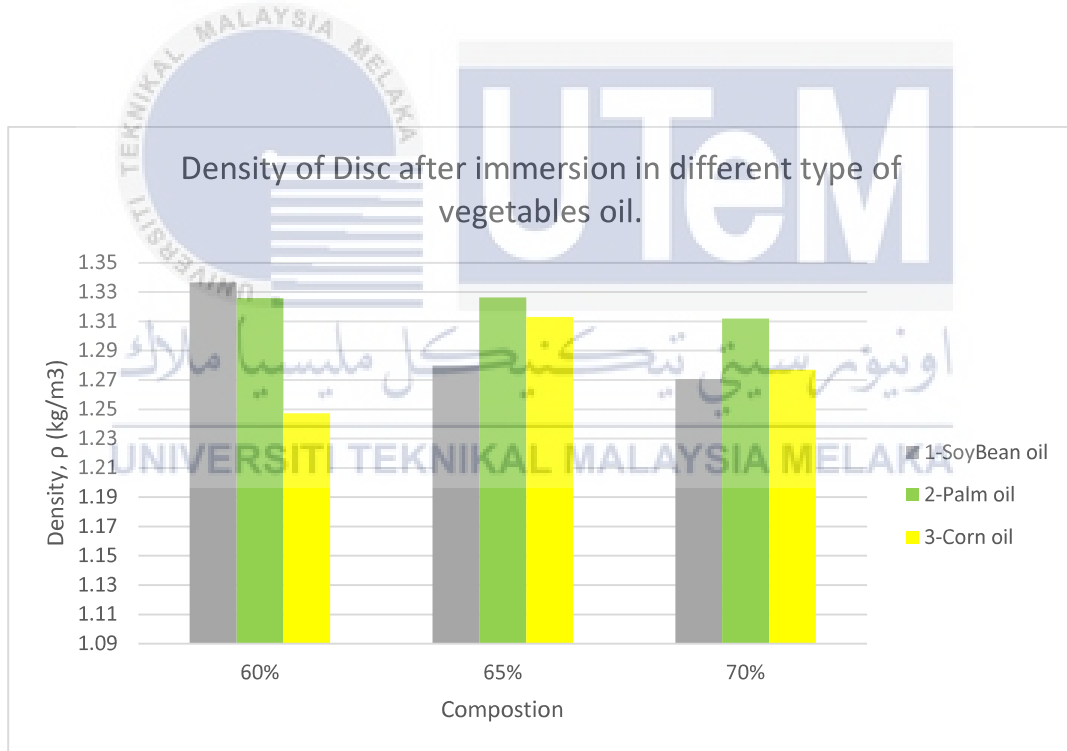


Figure 4-6: Density of disc after immersion in different type of vegetables oil.

Based on table 4-5, sample with composition of 60% of PKAC have average density of 1.294 kg/m³, for 65% has average density of 1.293 kg/m³ and 70% has average of 1.209

kg/m³. Sample with 60% composition of PKAC have highest average of density than 65% and 70%. Comparison between before and after immersing in different type of vegetables oil can obtained with table 4-5 and figure 4-6. All the sample increase in density after immersing in vegetables except for 65% composition immerse in soybean with decreasing 0.5%.

It was observed that increasing the amount of epoxy matrix increased the density. Due to the low interfacial bond between the carbon particles and the epoxy, the density began to decrease after a content ratio of 70%. The increase in density is caused by better interfacial adhesion with epoxies and a reduction in micro voids in the composite.(Mohmad et al., 2018).

4.4. Water absorption.

All the disc shape sample was immersed in water for 24 hours. Measure the weight of the sample before and after immersion. Then calculate the water absorption by using formula: $WA = \frac{Weight\ after - Weight\ before}{Weight\ before} \times 100$. All the data was recorded and tabulated in figure below.

Table 4-7: Water absorption of disc before immersion in different type of vegetables oil.

Composition	Sample No.	Water Absorption (%)
60%	1	0.028
	2	0.131
	3	1.530
65%	1	0.428
	2	0.003
	3	0.175
70%	1	4.911
	2	9.324
	3	12.688

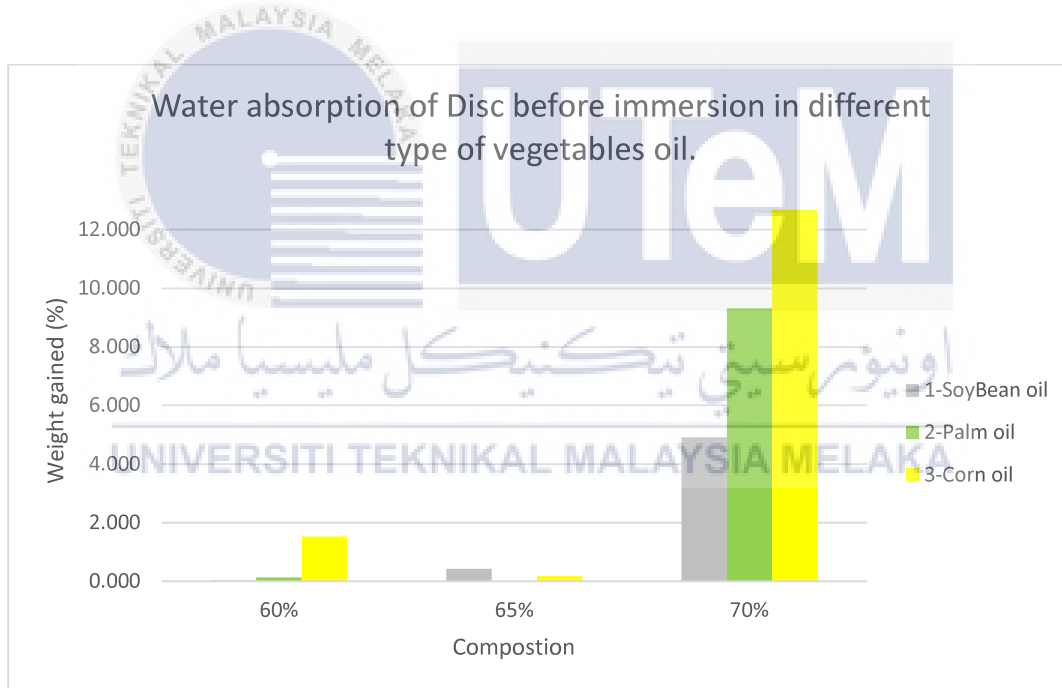


Figure 4-7: Water absorption of Disc before immersion in different type of vegetables oil.

Table 4-8: Water absorption of Disc after immersion in different type of vegetables oil.

Composition	Sample No.	Water Absorption
60%	1	-0.047
	2	0.076
	3	2.231
65%	1	0.736
	2	0.011
	3	0.290
70%	1	8.971
	2	14.947
	3	16.787

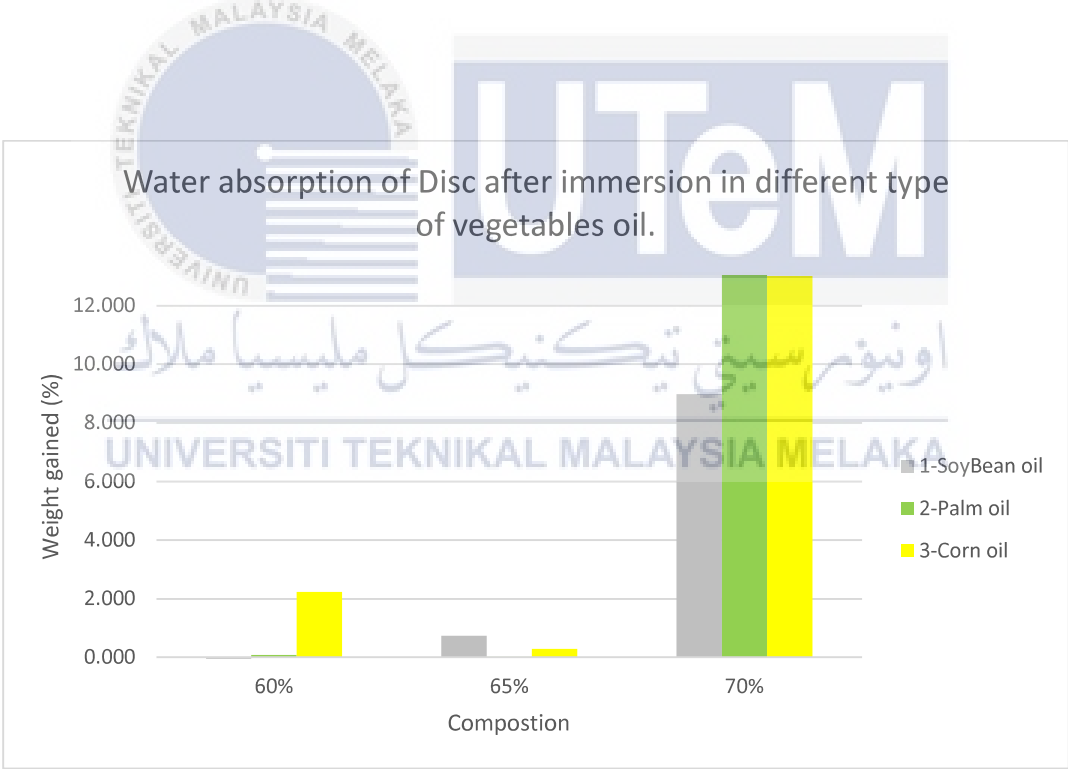


Figure 4-8: Water absorption of Disc after immersion in different type of vegetables oil.

Based on the table 4-7, sample with composition of 60% of PKAC water absorption of 0.563, for 65% has average water absorption of 0.202 and 70% has average of 8.974. Sample with composition of 70% PKAC has the highest value of water absorption than other composition which is 60% and 65%. Comparison between before and after immersion in different type of vegetables oil can obtained with table 4-7 and figure 4-8. All the sample increase value of water absorption except for composition 60% of PKAC with soybean and palm oil.

The density and void content material of the composite have a great effect at the rate of water absorption. As a result, because the activated carbon content material withinside the composite increase and the epoxy resin decreased, the water absorption rate increased, which can be attributed to the manufacturing of voids in the composite, which caused the formation of inner microchannels in the specimens. (Mohmad et al., 2018).



4.5. Porosity.

The porosity test was measured by obtaining the weight of the sample before and after immersion in vegetables oil. The weight after immersion minus with weight before immersion and divided with weight before immersion. The formula used is: *porosity* =

$$\frac{\text{Weight after} - \text{Weight before}}{\text{Weight before}} \times 100.$$

Table 4-9: Porosity for disc sample.

Composition	Sample No.	Porosity
60%	1	0.206
	2	0.108
	3	1.625
65%	1	0.299
	2	0.245
	3	0.042
70%	1	7.599
	2	13.570
	3	15.080

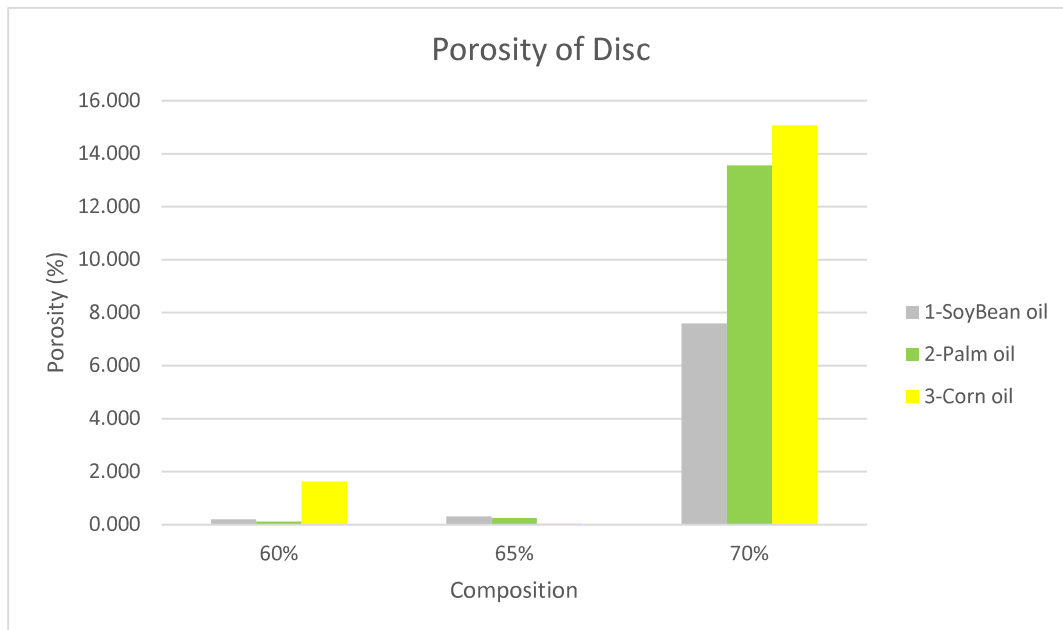


Figure 4-9: Porosity for disc sample.

Based on the figure 4-9, The average of porosity for 60% composition is 0.646, for 65% is 0.195 and 70% is 12.083. We can see huge different of porosity between sample with composition 70% and 60% and 65%. Because the sample had high interfacial bonding (60-40 percent), there were fewer voids, which allowed oil to enter the samples. oil molecules might enter the composite structure if the porosity of the polymeric composite increased.

Each composition of palm kernel activated carbon reinforced polymeric composite had a different porosity ratio. For each of them, the growing rate of porosity was significantly related to the reinforcement content, indicating that porosity grew proportionally with the amount of activated carbon in the composite until it reached its highest level with the 70-35 percent composite. Because of the saturation state of carbon with the epoxy resin and the development of bonds between them, this happened. Internal de-bonding and excessive porosity are also undesirable. To maintain the stability of composite dimensions, a high

degree of precision and high-quality adhesive bonding techniques are required (Mohmad et al., 2018).

4.6. Tensile test.

Tensile test was conducted based on ASTM D3039 / D3039M-17 standard using Instron universal testing machine. The speed of testing is 2mm/min. There are 12 samples going through this test which is 3 types of composition 60%, 65% and 70% for each category without oil, palm oil, soybean oil and corn oil. The data obtained tabulated below.

Table 4-10: Tensile strain.

Composition	Strain			
	Without oil	Palm oil	Soybean oil	Corn oil
60%	1.2476	0.8574	1.3048	1.3954
65%	1.0335	0.6763	0.7144	0.5097
70%	0.6477	0.6857	0.5810	0.1335

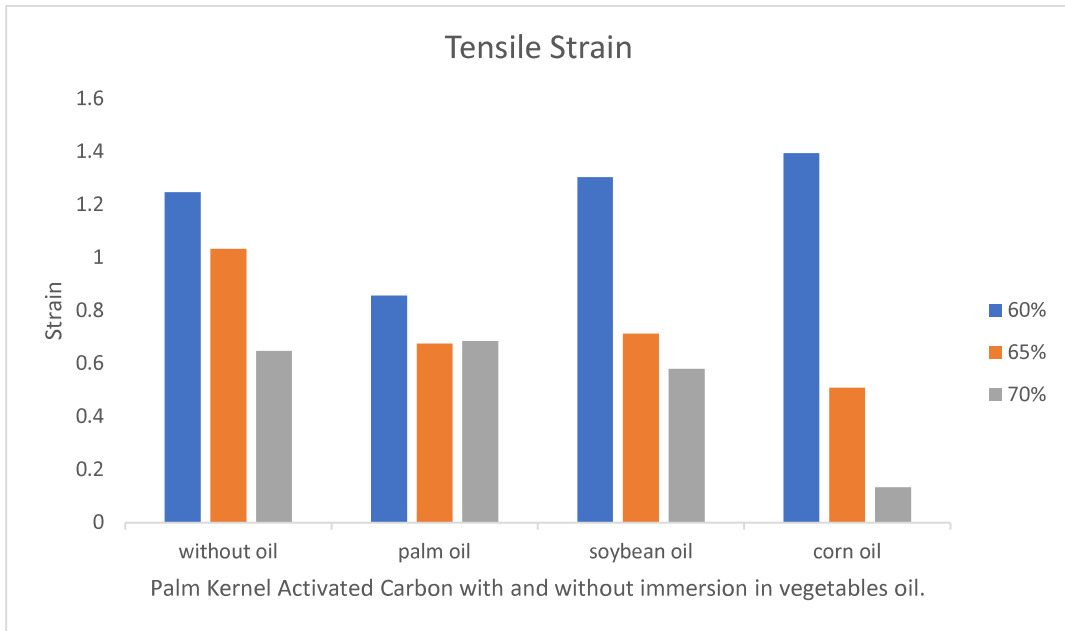


Figure 4-10: Tensile strain.

Table 4-11: Tensile stress.

Composition	Fracture stress, MPa			
	Without oil	Palm oil	Soybean oil	Corn oil
60%	17.9458	15.895	20.5209	23.5922
65%	15.2460	8.7848	8.6570	3.3694
70%	9.3406	5.4827	7.6982	1.7672

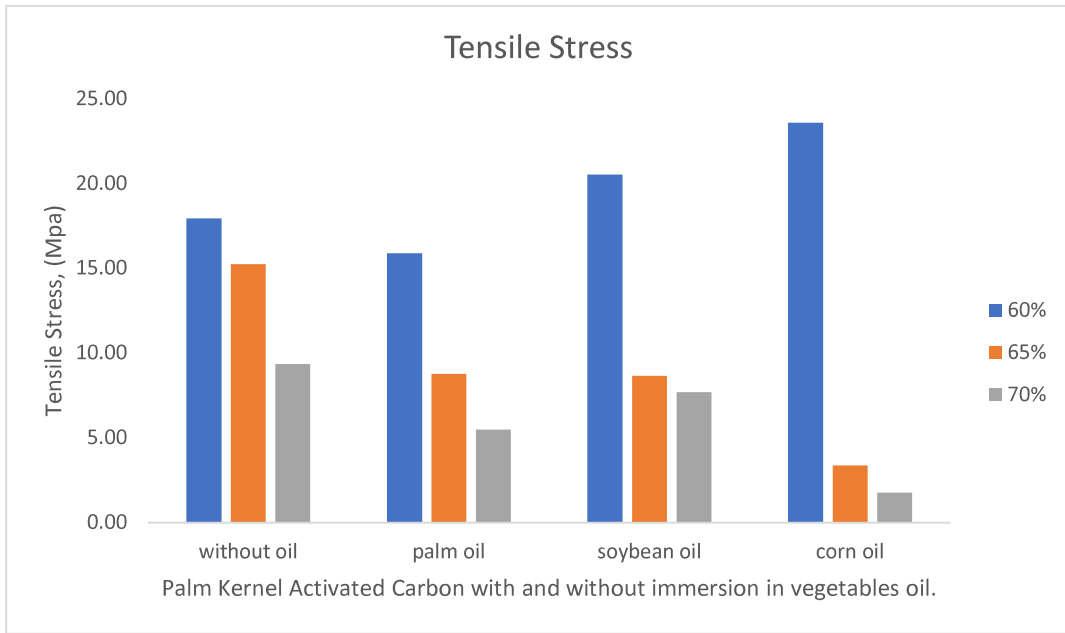


Figure 4-11: Tensile stress.

Table 4-12: Young modulus for tensile test.

Composition	Young modulus, MPa			
	Without oil	Palm oil	Soybean oil	Corn oil
60%	13.982	18.317	15.853	16.522
65%	13.685	13.754	12.171	6.6209
70%	14.491	7.6302	13.703	12.512

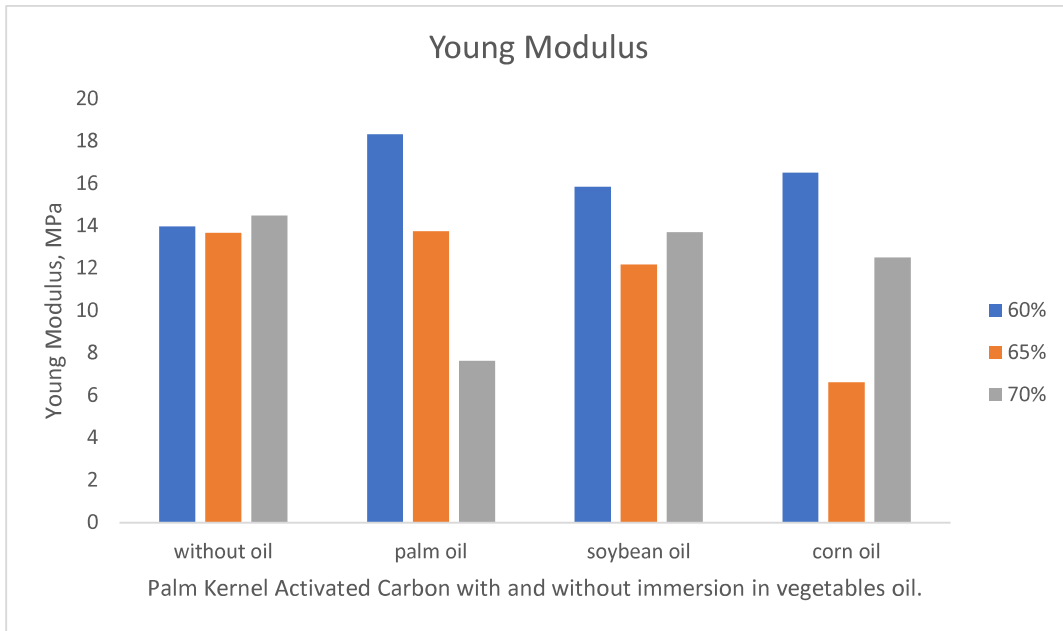


Figure 4-12: Young Modulus for tensile test.

The data obtained above shows comparison between PKAC samples with immersion in palm, soybean, and corn oil and without immersion in oil. For tensile test, composition 60% of PKAC have the greater value of tensile strain, tensile stress and young modulus compared to 65% and 70% composition. This is because of the higher carbon contents (70% and 65%) give the sample with lower rubber-like elasticity compared with lower carbon content (60%). In other words, the tensile stress increase when the concentration of the epoxy resin ratio increases between 60% of PKAC, because the epoxy strengthened the interface of the carbon material.

From table 4-11, it shows that 60% composition sample immersing in corn oil have the highest tensile stress value which is 23.5922MPa and palm oil has the lowest with 15.895MPa. For 65% composition sample, the highest tensile stress is without immerse in oil with 15.4260MPa and the lowest is corn oil with 3.3694MPa. For 70%, the highest tensile

stress is without immersion in oil with 9.3406MPa and the lowest is corn oil with 1.7672MPa. The data obtained are not constant which means the tensile stress when immerse in corn oil have the highest for 60% composition but the lowest for 65% and 70% composition. The value of tensile stress for 60% composition are slightly difference with immersion in 3 different oil and without immersion compared to composition 70% which have much difference between immersion in oil and without immersion. This is because the composition 70% absorb more oil because the porosity is greater than other composition. The existent of voids in 70% composition allows the oil to stay inside the sample and gives difference value of fracture stress.

According to Arash et al. (2015), increasing the weight % or ratio of a composite can improve its elastic modulus. Unfortunately, increasing amount of activated carbon make the value of elastic modulus decrease. This could have been caused by the particles' weak interfacial bonding. Elastic modulus is mostly affected by the interfacial adhesive bond, according to Uygunoglu et al. (2015). It could also have been caused by the high dispersion of voids induced by the use of modest volumes of epoxy resin to hold the activated carbon particle.

4.7. Compression test.

Compression test was conducted based on ASTM D6641 standard using Instron universal testing machine. The speed of testing is 2.5mm/min. There are 12 samples going through this test which is 3 types of composition 60%, 65% and 70% for each category without oil, palm oil, soybean oil and corn oil. The data obtained tabulated below.

Table 4-13: Compressive strain.

Composition	Strain			
	Without oil	Palm oil	Soybean oil	Corn oil
60	0.05	0.06	0.04	0.05
65	0.08	0.06	0.05	0.11
70	0.05	0.06	0.06	0.05

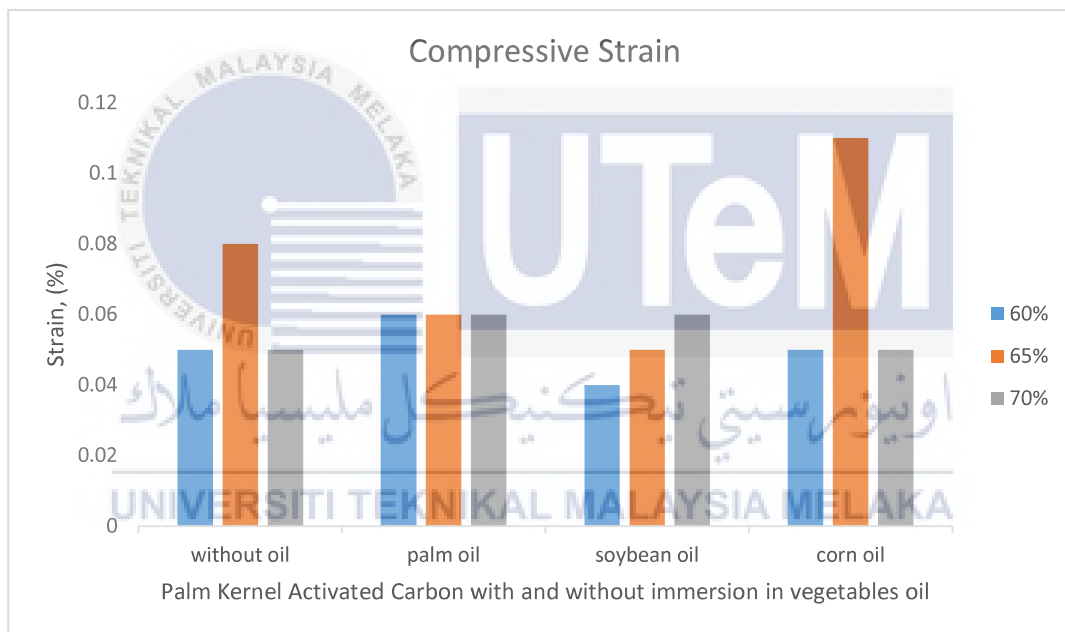


Figure 4-13: Strain for compression test.

Table 4-14: Compressive stress.

Composition	Compressive stress, MPa			
	Without oil	Palm oil	Soybean oil	Corn oil
60	120.93	123.64	85.92	121.22
65	64.02	113.67	96.93	79.06
70	105.29	96.13	100.13	107.39

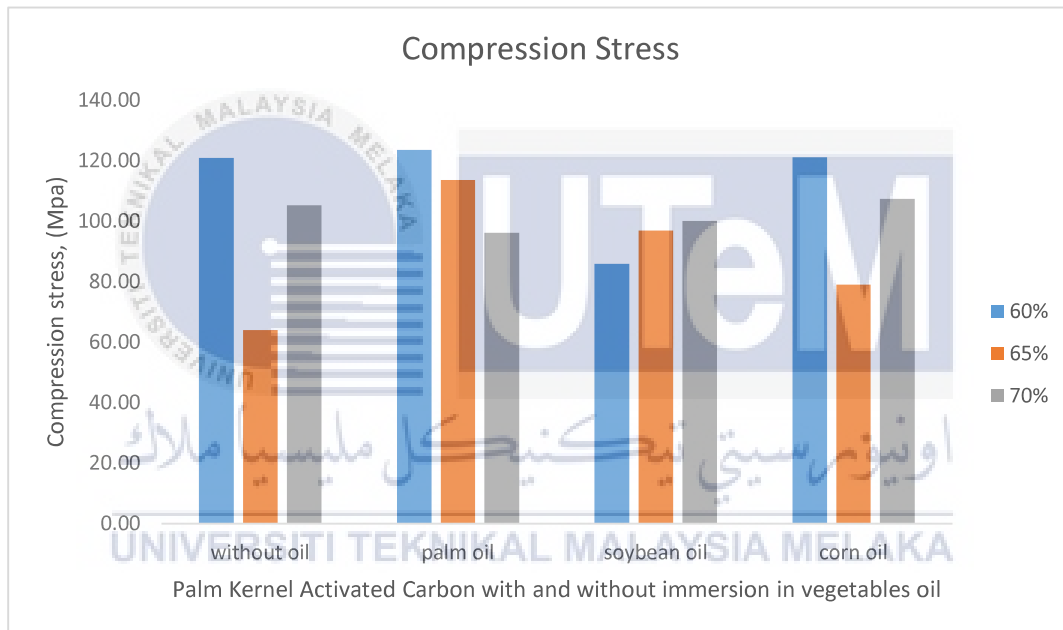


Figure 4-14: Compression stress.

Table 4-15: Young modulus for compression test.

Composition	Young Modulus, MPa			
	Without oil	Palm oil	Soybean oil	Corn oil
60	3180.0	3015.1	2418.3	3069.9
65	1555.9	2099.9	2379.9	2619.9
70	2557.6	1998.9	1964.0	2617.4

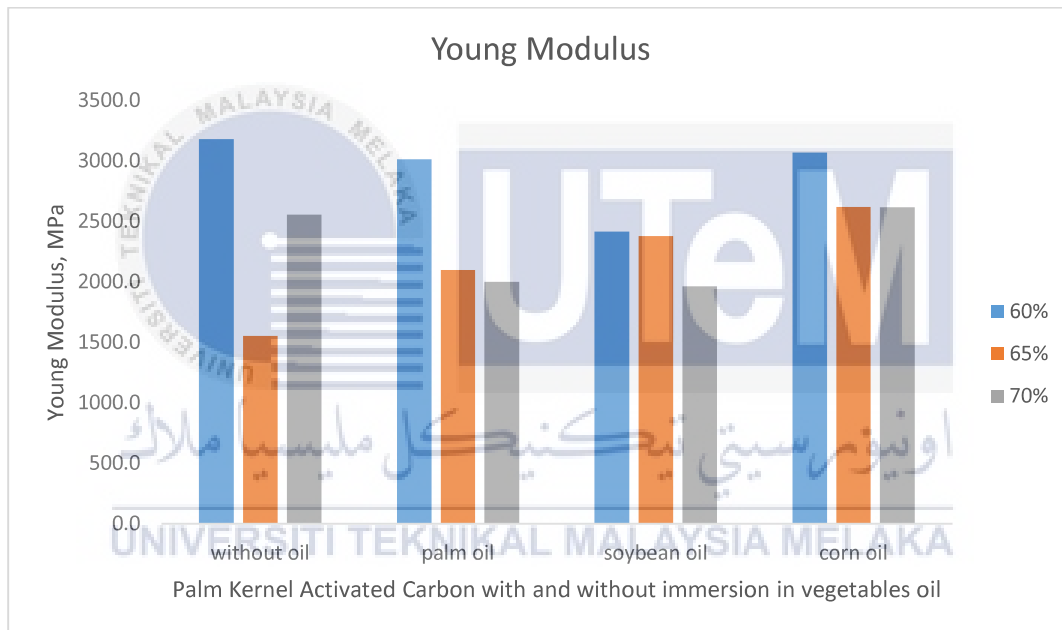
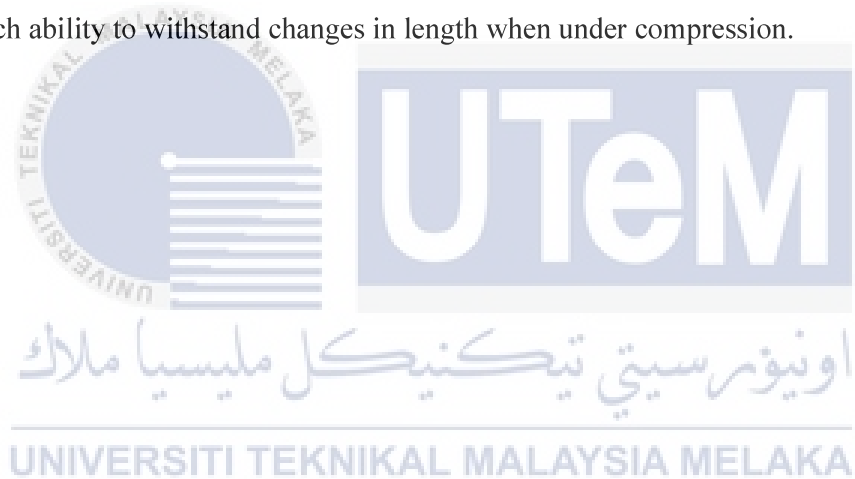


Figure 4-15: Young modulus for compression test.

The data obtained above shows comparison between PKAC samples with immersion in palm, soybean, and corn oil and without immersion in oil. For compression test, composition 60% of PKAC have the greater value of strain, fracture stress and young modulus compared to 65% and 70% composition. From table 4-14, it shows that 60%

composition immersion in palm oil have the highest compressive stress value which is 123.64MPa and soybean oil has the lowest with 85.92MPa. For 65% composition, the highest compressive stress is palm oil with 113.67MPa and the lowest is without oil with 64.02MPa. For 70%, the highest compressive stress is corn oil with 107.39MPa and the lowest is palm oil with 96.13MPa.

The data obtained are not constant which means the compressive stress when immerse in palm oil have the highest for 60% composition but the lowest for 70% composition. Based on table 4-15, the young modulus for sample immersed in corn oil have the high values for all the composition 60%, 65% and 70%. This mean sample with corn oil have much ability to withstand changes in length when under compression.



CHAPTER 5

CONCLUSION AND RECOMMENDATION

In conclusion, it was observed that the composition of 60% of palm kernel activated carbon was the best composition of composite in term of physical and mechanical properties compared to 65% and 70% composition. This is because the greater number of PKAC and lower number of epoxies in the sample cause of weak interfacial bonding between the particles and high distribution of voids. It can be shown in water absorption test where the percentage is highest for 70% composition. The poor resistance of reinforcement fillers to water absorption effects the mechanical properties and dimensional stability.

24 hours immersion of the PKAC into different types of vegetables oil give slightly different on physical properties. Some of the data obtained give increment on physical and mechanical value after immersing in vegetables oil. Also, some of the data give decline after immersion. Majority of the sample gives increment value of physical and mechanical properties after immersion in vegetables oil compared to before immersion.

For recommendation, the difference on the physical properties and mechanical properties not to significantly. By increasing the time of immersion into vegetables oil will give different results that are better for the physical and mechanical properties. As we know that composition 60% is the best in both physical and mechanical properties, we can select this composition to make research about other properties in future study.

REFERENCES

- Abdullah, A., Jamaludin, S. B., Noor, M. M., & Hussin, K. (2011). Composite cement reinforced coconut fiber: Physical and mechanical properties and fracture behavior. *Australian Journal of Basic and Applied Sciences*, 5(7), 1228–1240.
- Arash, B., Park, H. S., & Rabczuk, T. (2015). Tensile fracture behavior of short carbon nanotube reinforced polymer composites: A coarse-grained model. *Composite Structures*, 134, 981–988. <https://doi.org/10.1016/j.compstruct.2015.09.001>
- Bakry, M., Mousa, M. O., & Ali, W. Y. (2013). Friction and wear of friction composites reinforced by natural fibres. *Materialwissenschaft Und Werkstofftechnik*, 44(1), 21–28. <https://doi.org/10.1002/mawe.201300962>
- Banakar, P., Shivananda, H. K., & Niranjana, H. B. (2012). Influence of Fiber Orientation and Thickness on Tensile Properties of Laminated Polymer Composites. *International Journal of Pure and Applied Sciences and Technology*, 9(1), 61–68.
- Berman, D., Erdemir, A., & Sumant, A. V. (2014). Graphene: A new emerging lubricant. *Materials Today*, 17(1), 31–42. <https://doi.org/10.1016/j.mattod.2013.12.003>
- Bewilogua, K., & Hofmann, D. (2014). History of diamond-like carbon films - From first experiments to worldwide applications. *Surface and Coatings Technology*, 242, 214–225. <https://doi.org/10.1016/j.surfcoat.2014.01.031>
- Brostow, W., Kovačević, V., Vrsaljko, D., & Whitworth, J. (2010). Tribology of polymers and polymer-based composites. *Journal of Materials Education*, 2010(Vol.32 (5-6): 273-290), 273–290. 2010 Tribology of polymers and polymer-based composites_UNT_EDU_.pdf
- Bryant, P. J., Gutshall, P. L., & Taylor, L. H. (1964). A study of mechanisms of graphite

friction and wear. *Wear*, 7(1), 118–126. [https://doi.org/10.1016/0043-1648\(64\)90083-3](https://doi.org/10.1016/0043-1648(64)90083-3)

Chen, W., Yu, Y., Cheng, J., Wang, S., Zhu, S., Liu, W., & Yang, J. (2018). Microstructure, Mechanical Properties and Dry Sliding Wear Behavior of Cu-Al₂O₃-Graphite Solid-Lubricating Coatings Deposited by Low-Pressure Cold Spraying. *Journal of Thermal Spray Technology*, 27(8), 1652–1663. <https://doi.org/10.1007/s11666-018-0773-4>

Chua, K. W., Abdollah, M. F. B., Ismail, N., & Amiruddin, H. (2014). Potential of palm kernel activated carbon epoxy (PKAC-E) composite as solid lubricant: Effect of load on friction and wear properties. *Jurnal Tribologi*, 2(July), 31–38. http://jurnaltribologi.mytribos.org/v2/v2_2.html

Cui, L., Lu, Z., & Wang, L. (2014). Probing the low-friction mechanism of diamond-like carbon by varying of sliding velocity and vacuum pressure. *Carbon*, 66, 259–266. <https://doi.org/10.1016/j.carbon.2013.08.065>

Descartes, S., Saulot, A., Godeau, C., Bondeux, S., Dayot, C., & Berthier, Y. (2011). Wheel flange/rail gauge corner contact lubrication: Tribological investigations. *Wear*, 271(1–2), 54–61. <https://doi.org/10.1016/j.wear.2010.10.019>

Donnet, C. (1996). Advanced solid lubricant coatings for high vacuum environments. *Surface and Coatings Technology*, 80(1–2), 151–156. [https://doi.org/10.1016/0257-8972\(95\)02702-5](https://doi.org/10.1016/0257-8972(95)02702-5)

Donnet, C., & Grill, A. (1997). Friction control of diamond-like carbon coatings. *Surface and Coatings Technology*, 94–95, 456–462. [https://doi.org/10.1016/S0257-8972\(97\)00275-2](https://doi.org/10.1016/S0257-8972(97)00275-2)

Enke, K., Dimigen, H., & Hübsch, H. (1980). Frictional properties of diamondlike carbon layers. *Applied Physics Letters*, 36(4), 291–292. <https://doi.org/10.1063/1.91465>

- Hadoun, H., Sadaoui, Z., Souami, N., Sahel, D., & Toumert, I. (2013). Characterization of mesoporous carbon prepared from date stems by H₃PO₄ chemical activation. *Applied Surface Science*, 280, 1–7. <https://doi.org/10.1016/j.apsusc.2013.04.054>
- Hardwick, C., Lewis, R., & Olofsson, U. (2014). Low adhesion due to oxide formation in the presence of salt. *Proceedings of the Institution of Mechanical Engineers, Part F: Journal of Rail and Rapid Transit*, 228(8), 887–897. <https://doi.org/10.1177/0954409713495666>
- Jin, Y., Ishida, M., & Namura, A. (2011). Experimental simulation and prediction of wear of wheel flange and rail gauge corner. *Wear*, 271(1–2), 259–267. <https://doi.org/10.1016/j.wear.2010.10.032>
- Joshi, S., Adhikari, M., & Pradhananga, R. R. (2013). Adsorption of Fluoride Ion onto Zirconyl-Impregnated Activated Carbon Prepared from Lapsi Seed Stone. *Journal of Nepal Chemical Society*, 30, 13–23. <https://doi.org/10.3126/jncs.v30i0.9330>
- Kalin, M., Velkavrh, I., Vižintin, J., & Ožbolt, L. (2008). Review of boundary lubrication mechanisms of DLC coatings used in mechanical applications. *Meccanica*, 43(6), 623–637. <https://doi.org/10.1007/s11012-008-9149-z>
- La Mantia, F. P., & Morreale, M. (2011). Green composites: A brief review. *Composites Part A: Applied Science and Manufacturing*, 42(6), 579–588. <https://doi.org/10.1016/j.compositesa.2011.01.017>
- Lettington, A. H. (1998). Applications of diamond-like carbon thin films. *Carbon*, 36(5–6), 555–560. [https://doi.org/10.1016/S0008-6223\(98\)00062-1](https://doi.org/10.1016/S0008-6223(98)00062-1)
- Lewis, R., & Dwyer-Joyce, R. S. (2004). Wear mechanisms and transitions in railway wheel steels. *Proceedings of the Institution of Mechanical Engineers, Part J: Journal of Engineering Tribology*, 218(6), 467–478. <https://doi.org/10.1243/1350650042794815>

- Lewis, R., & Olofsson, U. (2004). Mapping rail wear regimes and transitions. *Wear*, 257(7–8), 721–729. <https://doi.org/10.1016/j.wear.2004.03.019>
- Lewis, Roger, & Olofsson, U. (2009). Basic tribology of the wheel-rail contact. In *Wheel-Rail Interface Handbook*. Woodhead Publishing Limited. <https://doi.org/10.1533/9781845696788.1.34>
- Li, W., Zheng, S., Cao, B., & Ma, S. (2011). Friction and wear properties of ZrO₂/SiO₂ composite nanoparticles. *Journal of Nanoparticle Research*, 13(5), 2129–2137. <https://doi.org/10.1007/s11051-010-9970-x>
- Mak, S. M., Tey, B. T., Cheah, K. Y., Siew, W. L., & Tan, K. K. (2009). Porosity characteristics and pore developments of various particle sizes palm kernel shells activated carbon (PKSAC) and its potential applications. *Adsorption*, 15(5–6), 507–519. <https://doi.org/10.1007/s10450-009-9201-x>
- Mat Tahir, N. A., Abdollah, M. F. Bin, Hasan, R., & Amiruddin, H. (2016). The effect of sliding distance at different temperatures on the tribological properties of a palm kernel activated carbon-epoxy composite. *Tribology International*, 94, 352–359. <https://doi.org/10.1016/j.triboint.2015.10.001>
- Menezes, P. L., Ingole, S. P., Nosonovsky, M., Kailas, S. V., & Lovell, M. R. (2013). Tribology for scientists and engineers: From basics to advanced concepts. *Tribology for Scientists and Engineers: From Basics to Advanced Concepts*, 9781461419, 1–948. <https://doi.org/10.1007/978-1-4614-1945-7>
- Mitchell, P. C. H. (1984). Oil-soluble MO-S compounds as lubricant additives. *Wear*, 100(1–3), 281–300. [https://doi.org/10.1016/0043-1648\(84\)90017-6](https://doi.org/10.1016/0043-1648(84)90017-6)
- Mohmad, M., Fadzli, M., Abdollah, B., Khudhair, A. Q., Tamaldin, N., Amiruddin, H., & Mohamad Zin, M. R. (2018). Physical-mechanical properties of palm kernel activated

- carbon reinforced polymeric composite : Potential as a self-lubricating material. *Jurnal Tribologi*, 17(April), 77–92.
- Najar, K. A. (2017). A Comparative Investigation Of Mechanical And Tribological Properties Of Multilayered CVD-Diamond Coatings: Effect Of Boron Doping. *Advanced Materials Letters*, 8(9), 932–938. <https://doi.org/10.5185/amlett.2017.6959>
- Nayani, M., Gunashekar, S., & Abu-zahra, N. (2013). *Synthesis and Characterization of Polyurethane-Nanoclay Composites*. 2013.
- Nilsson, R., Dwyer-Joyce, R. S., & Olofsson, U. (2006). Abrasive wear of rolling bearings by lubricant borne particles. *Proceedings of the Institution of Mechanical Engineers, Part J: Journal of Engineering Tribology*, 220(5), 429–439. <https://doi.org/10.1243/13506501J00205>
- Olofsson, U., & Telliskivi, T. (2003). Wear, plastic deformation and friction of two rail steels - A full-scale test and a laboratory study. *Wear*, 254(1–2), 80–93. [https://doi.org/10.1016/S0043-1648\(02\)00291-0](https://doi.org/10.1016/S0043-1648(02)00291-0)
- Olofsson, Ulf, Zhu, Y., Abbasi, S., Lewis, R., & Lewis, S. (2013). Tribology of the wheel-rail contact-aspects of wear, particle emission and adhesion. *Vehicle System Dynamics*, 51(7), 1091–1120. <https://doi.org/10.1080/00423114.2013.800215>
- Ostermeyer, G. P., & Müller, M. (2008). New insights into the tribology of brake systems. *Proceedings of the Institution of Mechanical Engineers, Part D: Journal of Automobile Engineering*, 222(7), 1167–1200. <https://doi.org/10.1243/09544070JAUTO595>
- Rahaman, M. L., Zhang, L., Liu, M., & Liu, W. (2015). Surface roughness effect on the friction and wear of bulk metallic glasses. *Wear*, 332–333, 1231–1237. <https://doi.org/10.1016/j.wear.2014.11.030>
- Reeves, C. J., Menezes, P. L., Jen, T. C., & Lovell, M. R. (2012). Evaluating the tribological

- performance of green liquid lubricants and powder additives based green liquid lubricants. Society of Tribologists and Lubrication Engineers Annual Meeting and Exhibition 2012, 62–64.
- Rymuza, Z. (2007). Tribology of polymers. *Archives of Civil and Mechanical Engineering*, 7(4), 177–184. [https://doi.org/10.1016/S1644-9665\(12\)60235-0](https://doi.org/10.1016/S1644-9665(12)60235-0)
- Shankar, S., Wang, L. F., & Rhim, J. W. (2017). Preparation and properties of carbohydrate-based composite films incorporated with CuO nanoparticles. *Carbohydrate Polymers*, 169, 264–271. <https://doi.org/10.1016/j.carbpol.2017.04.025>
- Shuhimi, F. F., Abdollah, M. F. Bin, Kalam, M. A., Hassan, M., Mustafa, A., & Amiruddin, H. (2016). Tribological characteristics comparison for oil palm fibre/epoxy and kenaf fibre/epoxy composites under dry sliding conditions. *Tribology International*, 101, 247–254. <https://doi.org/10.1016/j.triboint.2016.04.020>
- Song, J., Liu, X., Zhao, G., Ding, Q., & Qiu, J. (2019). Effect of surface roughness and reciprocating time on the tribological properties of the polyimide composites. *Polymer Engineering and Science*, 59(3), 483–489. <https://doi.org/10.1002/pen.24948>
- Spiryagin, M., Lee, K. S., Yoo, H. H., Kashura, O., & Popov, S. (2010). Numerical calculation of temperature in the wheel-rail flange contact and implications for lubricant choice. *Wear*, 268(1), 287–293. <https://doi.org/10.1016/j.wear.2009.08.014>
- Sundh, J., & Olofsson, U. (2008). Seizure mechanisms of wheel-rail contacts under lubricated conditions using a transient ball-on-disc test method. *Tribology International*, 41(9–10), 867–874. <https://doi.org/10.1016/j.triboint.2007.12.011>
- Tahir, N. A. M., Abdollah, M. F. Bin, Hasan, R., & Amiruddin, H. (2015). The effect of temperature on the tribological properties of palm kernel activated carbon-epoxy composite. *Tribology Online*, 10(6), 428–433. <https://doi.org/10.2474/trol.10.428>

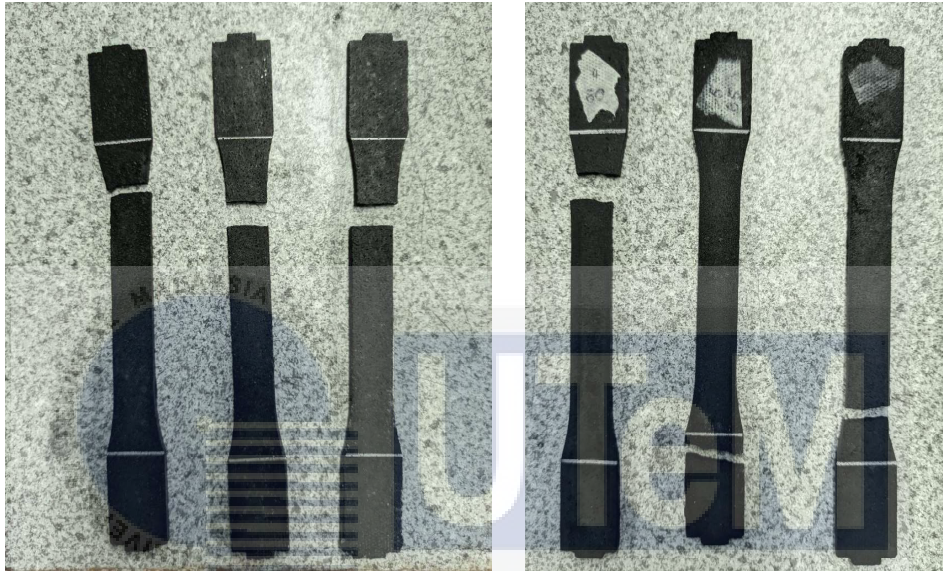
- Takano, A. (1999). Tribology-related space mechanism anomalies and the newly constructed high-vacuum mechanism test facilities in NASDA. *Tribology International*, 32(11), 661–671. [https://doi.org/10.1016/S0301-679X\(99\)00091-2](https://doi.org/10.1016/S0301-679X(99)00091-2)
- Tomeoka, M., Kabe, N., Tanimoto, M., Miyauchi, E., & Nakata, M. (2002). Friction control between wheel and rail by means of on-board lubrication. *Wear*, 253(1–2), 124–129. [https://doi.org/10.1016/S0043-1648\(02\)00091-1](https://doi.org/10.1016/S0043-1648(02)00091-1)
- Tzanakis, I., Hadfield, M., Thomas, B., Noya, S. M., Henshaw, I., & Austen, S. (2012). Future perspectives on sustainable tribology. *Renewable and Sustainable Energy Reviews*, 16(6), 4126–4140. <https://doi.org/10.1016/j.rser.2012.02.064>
- Uvaraja, V. C., Natarajan, N., Rajendran, I., & Sivakumar, K. (2013). Tribological behavior of novel hybrid composite materials using Taguchi technique. *Journal of Tribology*, 135(2), 1–12. <https://doi.org/10.1115/1.4023147>
- Uygunoglu, T., Gunes, I., & Brostow, W. (2015). Physical and mechanical properties of polymer composites with high content of wastes including boron. *Materials Research*, 18(6), 1188–1196. <https://doi.org/10.1590/1516-1439.009815>
- Verma, S., Kumar, V., & Gupta, K. D. (2012). Performance analysis of flexible multirecess hydrostatic journal bearing operating with micropolar lubricant. *Lubrication Science*, 24(6), 273–292. <https://doi.org/10.1002/ls>
- Yang, H., Cui, H., Tang, W., Li, Z., Han, N., & Xing, F. (2017). A critical review on research progress of graphene/cement based composites. *Composites Part A: Applied Science and Manufacturing*, 102, 273–296. <https://doi.org/10.1016/j.compositesa.2017.07.019>
- Zhou, J., Yang, J., Zhang, Z., Liu, W., & Xue, Q. (1999). Study on the structure and tribological properties of surface-modified Cu nanoparticles. *Materials Research Bulletin*, 34(9), 1361–1367. [https://doi.org/10.1016/S0025-5408\(99\)00150-6](https://doi.org/10.1016/S0025-5408(99)00150-6)

Zhu, Y. (2011). ZHU, Y. Adhesion in the wheel-rail contact under contaminated conditions. Stockholm, 2011. Diplomová práce. Royal Institute of Technology. Department of Machine Design. Vedoucí práce Prof. Ulf Olofsson.



APPENDICES

APPENDIX A1



APPENDIX A2



اونيورسيتي تېكنيكل مليسيا ملاك
UNIVERSITI TEKNIKAL MALAYSIA MELAKA

APPENDIX A3

